Role of UCHL1 in Regulating Gene Expression in Prostate Cancer Cells

by

Aleksandar Ilic

A Thesis submitted to the Faculty of Graduate Studies of

The University of Manitoba

in partial fulfilment of the requirements of the degree of

MASTER OF SCIENCE

Department of Biochemistry & Medical Genetics

University of Manitoba

Winnipeg

Abstract

Ubiquitin C-terminal hydrolase L1 (UCHL1) is a multifunctional protein primarily expressed in neuronal cells and involved in numerous cellular processes. UCHL1 has been linked with neurodegenerative diseases and a wide range of cancers but its specific role remains unknown. Previous UCHL1 knockdown studies have shown that UCHL1 controls the expression of pro- and anti-apoptotic genes as well as genes involved in cell cycle regulation but it is unknown how UCHL1 regulates these genes.

We have shown that UCHL1 is cross-linked to DNA in DU145 but not in LNCaP or PC3 prostate cancer cells. Therefore, we hypothesized that UCHL1 regulates the expression of pro- or anti-apoptotic genes as well as the genes involved in the cell cycle through its interaction with DNA. By utilizing ChIP and ChIP-seq analyses it is possible to determine the UCHL1 target sequences on the genomic DNA.

It was shown that UCHL1 is only expressed in DU145 but not in LNCaP, PC3 or C4-2 prostate cancer cell lines. Additionally, UCHL1 is expressed and cross-linked to DNA in HEK293T cells. It is believed that UCHL1 is silenced by upstream promoter methylation when it is not expressed. However, treatment with the epigenetic drugs 5-aza-2′-deoxycytidine and trichostatin A (TSA) did not result in induction of UCHL1 expression in LNCaP, PC3 or C4-2 prostate cancer cell lines.

UCHL1 is also associated with p53. However, ChIP assay results have shown that UCHL1 and p53 do not bind to genomic DNA of upstream promoter regions *CDKN1A* and *BAX* genes. Additionally, through UCHL1 ChIP-seq analyses in DU145 and HEK293T cells, we discovered that UCHL1 co-localizes to the DNA with the shelterin complex shedding light on a new role of UCHL1 that has never been described before.

Acknowledgments

Firstly, I would like to thank my supervisor and mentor Dr Jim Davie. I am very grateful for the opportunity he has given me. His vast knowledge, experience and patience throughout my studies were tremendously helpful. Similarly, his continuous guidance and advice helped me overcome any problems I encountered in my work.

Additionally, I would like to thank my committee members, Dr Kirk McManus, Dr Mojgan Rastegar and Dr Yvonne Myal. All of their time, suggestions and advice have been greatly appreciated.

Mrs. Tuntun Sarkar has been a very important person before and during my graduate studies. Her help was instrumental in enrolling in graduate studies and I am grateful for her support and helpful advice in the past three years.

I would like to thank all of the Davie lab members, both past and present. Par Kamaleswaran, Xuemei Wang, Nehal Patel, Protiti Khan and Golam Sabbir helped me learn many lab techniques when I first joined the lab and I am very appreciative. I would like to thank Dilshad Khan for all her assistance in learning the ChIP assay, which was essential in completing my lab work. A special thanks to Carolina Gonzalez-Zuluaga for all her help with sequencing as well as Debbie Tsuyuki and Wayne Xu. Also, I would like to thank lab managers Cheryl Peltier and Shihua He. Sanzida Jahan has been incredibly helpful throughout my studies. Also, thanks to all former Davie lab members: Shannon Healy, Soma Mandal, Kevin Cao, Patricija Zot, Jessica Jarmasz and Donna Lee.

Finally, I would like to thank my family, my parents Djordje and Tatjana and my sister Nataša. All of their love, support and words of encouragement throughout my studies were invaluable in completing my degree.

Table Of Contents

List of Tables

List of Figures

List of Copyrighted Material for Which Permission Was Obtained

List Of Abbreviations

°C	Degrees Celsius
2D	Two-dimensional
2D PAGE	Two-dimensional polyacrylamide gel electrophoresis
A_{260}	Absorbance at 260 nm
AD	Androgen dependent
AI	Androgen independent
APRT	Adenine Phosphoribosyltransferase
AR	Androgen receptor
AS	Androgen sensitive
ASXL1	Additional Sex Combs Like 1
ATCC	American Type Culture Collection
ATP	Adenosine triphosphate
BAP1	BRCA1 associated protein-1
BAX	BCL2-Associated X Protein
BCL2	B-cell CLL/lymphoma 2
BIK	BCL2-interacting killer (apoptosis-inducing)
bp	Base pairs
BRCA1	Breast cancer 1, early onset
BRCT	BRCA1 C-terminal
BSA	Bovine serum albumin
$CaCl_2$	Calcium chloride
CCLE	Cancer Cell Line Encyclopedia
CDK	Cyclin-dependent kinase
CDKN1A	Cyclin-Dependent Kinase Inhibitor 1A
CDKN1B	Cyclin-Dependent Kinase Inhibitor 1B
ChIP	Chromatin immunoprecipitation
ChIP-seq	Chromatin immunoprecipitation sequencing
CHRDL2	Chordin-like 2
CLIC6	Chloride intracellular channel 6
cm	Centimetre
Co-IP	Co-immunoprecipitation
CO_2	Carbon dioxide
COX2	Cyclooxygenase 2
CpG	Cytosine-phosphate-guanine
CRPC	Castration-resistant prostate cancer
ddH_2O	Double-distilled water
DDX11L2	DEAD/H (Asp-Glu-Ala-Asp/His) box helicase 11 like 2
DMEM	Dulbecco's modified Eagle's medium
DMSO	Dimethyl sulfoxide
DNA	Deoxyribonucleic acid
DNMT	DNA methyltransferase
DSP	Dithiobis[succinimidyl propionate]
DUB	Deubiquitinating enzyme
ECL	Enhanced chemiluminescence

EDTA	Ethylenediaminetetraacetic acid
EMEM	Eagle's minimal essential medium
EMT	Epithelial-to-mesenchymal transition
ENCODE	Encyclopedia of DNA Elements
ePCR	Emulsion polymerase chain reaction
FAM157A	Family with sequence similarity 157, member A
FBS	Fetal bovine serum
GST	Glutathione S-transferase
GSTP1	Glutathione S-transferase pi 1
HECT	Homologous to the E6-AP Carboxyl Terminus
HCF-1	Host cell factor 1
HCl	Hydrochloric acid
HDAC	Histone deacetylase
hINO80	Human INO80 complex subunit
ID	Immunodepleted
IF	Immunofluorescence
IgG	Immunoglobulin G
IGV	Integrative Genomics Viewer
IP	Immunoprecipitation
ITS	Interstitial telomeric sequence
JAB1	Jun Activation Domain-Binding Protein 1
JAMM	JAB1/MPN/Mov34 metalloprotease
KAT	Lysine acetyltransferase
KCl	Potassium chloride
kDa	Kilodalton
lncRNA	Long non-coding ribonucleic acid
LRP1B	Low density lipoprotein receptor-related protein 1B
M	Molar concentration
MBD	Methyl CpG-binding domain
MDM2	Mouse double minute 2 homolog
MET	Mesenchymal-to-epithelial transition
MJD	Machado-Josephin domain
mL	Millilitres
MLH1	MutL Homolog 1
mM	Millimolar concentration
MNase	Micrococcal nuclease
mRNA	Messenger ribonucleic acid
MYB	Myeloblastosis
N-ChIP	Native chromatin immunoprecipitation
NaCl	Sodium chloride
$NaHCO_3$	Sodium bicarbonate
NCBI	National center for biotechnology information
NEDD8	Neural Precursor Cell Expressed, Developmentally Down-Regulated 8
NF-κB	Nuclear Factor Of Kappa Light Polypeptide Gene Enhancer In B-Cells
ng	Nanograms
NGS	Next-generation sequencing

NHEJ	Non-homologous end joining
nM	Nanomolar concentration
NP-40	Octylphenoxypolyethoxyethanol
OTU	Ovarian tumour
PARK5	Parkinson's disease 5
PBS	Phosphate buffered saline
PcG	Polycomb-group
PCR	Polymerase chain reaction
PD	Parkinson's disease
PE	Paired-end
PGP9.5	Protein gene product 9.5
PIPES	Piperazine-N,N′-bis(2-ethanesulfonic acid)
PLXNB2	Plexin B2
PMSF	Phenylmethanesulfonylfluoride
POT1	Protection of telomeres
PR-DUB	Polycomb repressive-deubiquitinase
pRb	Retinoblastoma protein
PRDX1	Peroxiredoxin 1
PSA	Prostate-specific antigen
PTGS2	Prostaglandin-endoperoxide synthase 2
PTM	Posttranslational modification
qPCR	Real-time polymerase chain reaction
RAP1	Repressor/Activator protein 1
RASGRF1	Ras protein-specific guanine nucleotide-releasing factor 1
RHOA	Ras homolog family member A
RIPA	Radioimmunoprecipitation assay
RNA	Ribonucleic acid
RNA-seq	Ribonucleic acid sequencing
RNase A	Ribonuclease A
RPMI-1640	Roswell Park Memorial Institute 1640
RT-PCR	Reverse transcription polymerase chain reaction
SDS	Sodium dodecyl sulfate
SDS-PAGE	Sodium dodecyl sulfate polyacrylamide gel electrophoresis
SE	Single-end
SNP	Single nucleotide polymorphism
SOLiD	Sequencing by Oligonucleotide Ligation and Detection
SUMO	Small ubiquitin-like modifier
TBE	Tris Borate EDTA
TBST	Tris-buffered saline tween 20
TERF2IP	Telomeric Repeat Binding Factor 2, Interacting Protein
TFIIH	Transcription factor II Human
TIN2	TRF1-interacting nuclear factor 2
TINF2	TRF1-interacting nuclear factor 2
TPP1	POT1 and TIN2 interacting protein
TRANSFAC	Transcription factor database
TRF1	Telomeric repeat binding factor 1

TRF2	Telomeric repeat binding factor 2
TRFH	Telomeric repeat binding factor homology
TSA	Trichostatin A
U	Units
UCH	Ubiquitin C-terminal hydrolase
UCHL1	Ubiquitin C-terminal hydrolase L1
UCHL3	Ubiquitin C-terminal hydrolase L3
UCHL5	Ubiquitin C-terminal hydrolase L5
USP	Ubiquitin-specific proteases
V	Volts
v/v	Volume/volume
w/v	Mass/volume
X-ChIP	Cross-linking Chromatin Immunoprecipitation
xg	Centrifugal force
µg	Microgram
µL	Microlitre
µm	Micrometre

Chapter 1: Introduction

1.1 Ubiquitin C-Terminal Hydrolase L1 (UCHL1)

UCHL1 (ubiquitin C-terminal hydrolase L1) or PGP9.5 (protein gene product 9.5) is the most extensively studied protein of the UCH subclass of deubiquitinating enzymes. UCHL1 is a 223 amino acid protein and the shortest protein of the four UCH deubiquitinating proteases. Along with UCHL3, it has a highly knotted structure with five crossings where it folds over five times to create a knot (Figure 1) (Das *et al.,* 2006; Virnau *et al.,* 2006). UCHL1 is primarily expressed in neuronal cells, the pancreas (islets of Langerhans) and neuroendocrine cells (Day and Thompson, 2010). It is estimated that UCHL1 makes up 1-2% of total brain protein (Doran *et al.,* 1983). UCHL1 is also expressed at lower levels in the testis, kidney, ovary and large intestine but not in prostate (Day and Thompson, 2010). UCHL1 protein is highly conserved in evolution shedding light on its importance to numerous species (Das *et al.,* 2006; Day and Thompson, 2010).

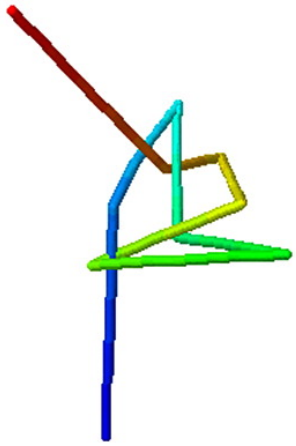

Figure 1. The 5_2 knotted structure of UCHL1. It has five crossings and folds over five times to create a knot (Day and Thompson, 2010).

The primary function of UCHL1 is believed to be the hydrolysis of esters and amides of the C-terminal of ubiquitin, thus producing monomeric ubiquitin (Wilkinson *et al.,* 1989). However, it is disputed whether UCHL1 is a true hydrolase due to its low hydrolase activity compared to other hydrolase enzymes (Das *et al.,* 2006; Day and Thompson, 2010). *In vitro* studies have also shown that UCHL1 has a dimerization-dependent ubiquitin ligase function through Lys-63 linkages. UCHL1 has been shown to have roles independent of its hydrolase or ligase function. It interacts and stabilizes mono-ubiquitin by increasing its half-life and inhibiting degradation thus playing a role in ubiquitin homeostasis (Osaka *et al.,* 2003). A recent study has also shown that UCHL1 interacts with cyclin-dependent kinases CDK1, CDK4, CDK5 and CDK6. This interaction is also independent of deubiquitinating activity. It is suggested that this is a novel role of UCHL1 in cell cycle regulation and cell proliferation (Kabuta *et al.,* 2013).

The potential roles of UCHL1 in disease still remain largely unknown. UCHL1 has been associated with various diseases but its specific roles are disputed and still generally undetermined. UCHL1 has been linked with diseases such as Parkinson's disease, Alzheimer's disease as well as a wide range of cancers.

1.2 UCHL1 and Deubiquitination

Deubiquitination is a process where deubiquitinating enzymes (DUBs) cleave isopeptide bonds between linked ubiquitin proteins or ubiquitin and target proteins by hydrolysis. DUBs can be divided into cysteine proteases or metalloenzymes. Deubiquitination by DUBs involves processing of ubiquitin precursors, hydrolysis of mono-ubiquitin from distal ends of poly-ubiquitin chains, deubiquitination of mono- or

poly- ubiquitin chains, processing of poly-ubiquitin chains at the proteasome and generating mono-ubiquitin (Figure 2) (Amerik and Hochstrasser, 2004; Kim *et al.,* 2003).

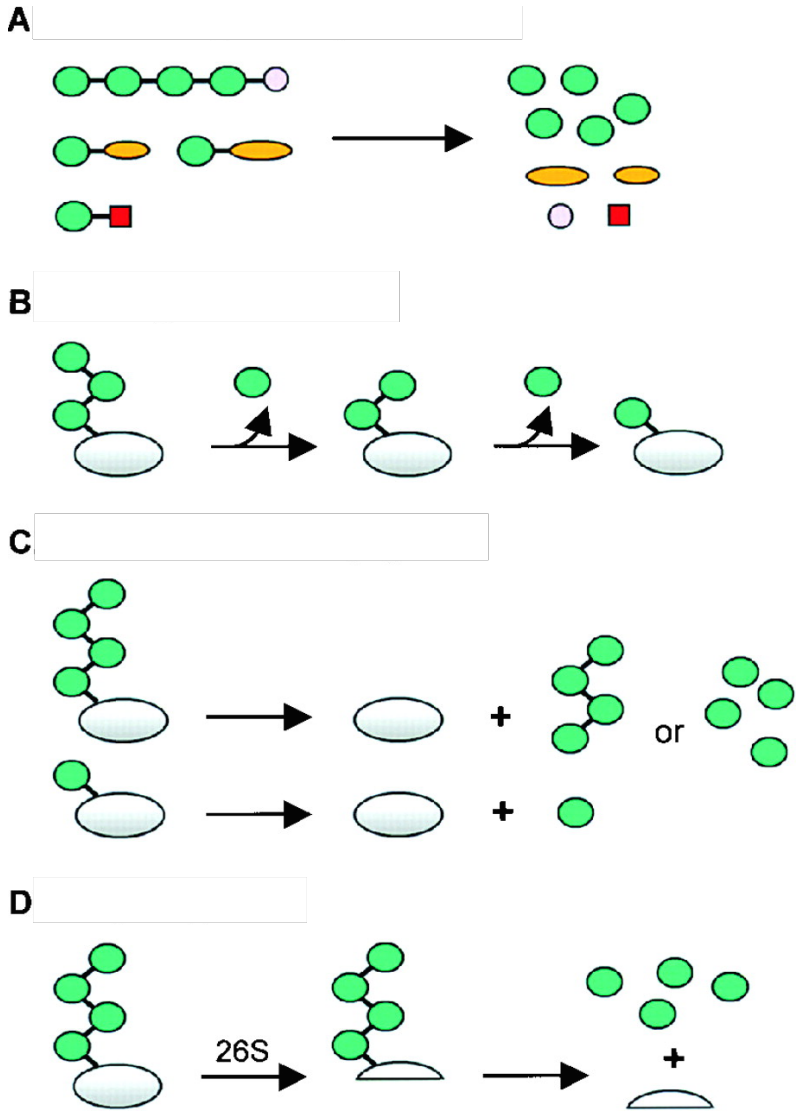

Figure 2. DUBs are involved in the processing of precursors of ubiquitin (A), hydrolysis of mono-ubiquitin from distal ends of poly-ubiquitin chains (B), deubiquitinating mono- or poly-ubiquitin chains (C) and processing of poly-ubiquitin chains at the proteasome (D). Ubiquitin is shown in green, the substrate proteins in white, single amino acids in pink, ribosomal fusion proteins in orange and ubiquitin adducts in red (Kim *et al.,* 2003).

Cysteine proteases can further be divided into four subclasses based of their ubiquitin protease catalytic domains. These subclasses include ubiquitin-specific proteases (USPs), ovarian tumour (OTU) proteases, Machado-Josephin domain (MJD)

proteases and ubiquitin C-terminal hydrolases (UCH). Deubiquitinating metalloproteases are all categorized into one class and all contain the JAMM (JAB1/MPN/MOV34) domain.

UCHL1 is classified into the ubiquitin C-terminal hydrolase (UCH) subclass of DUBs. Its role as a DUB is described in the hydrolysis of the C-terminal glycine of ubiquitin generating mono-ubiquitin. Apart from UCHL1, the UCH subclass of DUBs consists of three more proteins including UCHL3, UCHL5 and BAP1. All four UCH DUBs contain the UCH catalytic domain that contains the catalytic triad. The catalytic triad contains Cys-His-Asp residues and is conserved in this subclass (Amerik and Hochstrasser, 2004).

UCHL3 (ubiquitin C-terminal hydrolase L3) is a 230 amino acid protein and is most closely related to UCHL1, as they share a 53% sequence identity (Fang *et al.,* 2010). UCHL3 also has the highly knotted structure and is highly expressed in the heart, skeletal muscles and testis. Lower expression is shown in other tissues such as kidney and liver (Wada *et al.,* 1998). Besides ubiquitin hydrolysis, UCHL3 is able to process NEDD8, an ubiquitin-like protein that shares a 60% identity to ubiquitin (Wada *et al.,* 1998). UCHL3 can also hydrolyze a mutated form of ubiquitin, UBB^{+1}, which is associated with neurodegenerative disease (Dennissen *et al.,* 2011). UCHL3 was shown to interact with di-ubiquitin whereas UCHL1 interacts with mono-ubiquitin (Setsuie *et al.,* 2009). Unlike UCHL1, UCHL3 does not form dimers and hence does not have a dimerization-dependent ubiquitin ligase function (Liu *et al.,* 2002).

UCHL5 (ubiquitin C-terminal hydrolase L5) or UCH37 is a 329 amino acid protein that is ubiquitously expressed and not tissue-specific. It is rather unique when

compared to other proteases in the UCH subclass since it is the only UCH that is associated with the proteasome (Hamazaki *et al.,* 2006; Yao *et al.,* 2006). The 26S proteasome is a large protein complex comprised of the 20S proteasome and two 19S regulatory particles (Baumeister *et al.,* 1998). UCHL5 is part of the 19S regulatory particle that recognizes ubiquitinated proteins marked for proteasomal degradation.

BAP1 (BRCA1-associated protein 1) is the largest member of UCH subclass at 729 amino acids. BAP1 is localized to the nucleus and is highly expressed in placenta and testis. It is also expressed in the kidney, pancreas and ovary (Jensen *et al.,* 1998). As its name suggest, BAP1 was identified as a protein bound to the RING finger domain of BRCA1 (Eletr and Wilkinson, 2011). However, BAP1 does not deubiquitinate BRCA1 and therefore the function of BAP1 associated with BRCA1 still remains elusive (Mallery *et al.,* 2002; Nishikawa *et al.,* 2009).

1.3 UCHL1 and Ubiquitination

Ubiquitin is a small protein of 76 amino acids (8.5 kDa) that is conjugated to a target protein through the process of ubiquitination. It is a highly conserved protein in eukaryotes. This is especially evident by the fact that the human and yeast ubiquitin proteins differ in only three residues (Wilkinson, 2000). Substrate proteins are modified by the addition of ubiquitin and ubiquitin conjugation is important in many cellular processes. These include protein degradation, signal transduction, transcriptional regulation and protein localization (Hershko and Ciechanover, 1998; Schnell and Hicke, 2003).

Ubiquitination is a cellular process where ubiquitin is covalently attached to a target protein. Ubiquitin is conjugated to a target protein through a three-step ubiquitination process comprised of activation, conjugation and ligation. An E1 enzyme via an ATP-dependent step first activates ubiquitin. Then, ubiquitin is transferred to the E2 ubiquitin-conjugating enzyme. Lastly, an E3 ubiquitin-ligase facilitates the formation of an isopeptide bond between the C-terminal glycine residue of ubiquitin and the lysine residue of the substrate protein (Figure 3) (Husnjak and Dikic, 2012). Di- or poly-ubiquitination occurs by ligation of additional ubiquitin proteins to a lysine residue of ubiquitin already ligated to the target protein.

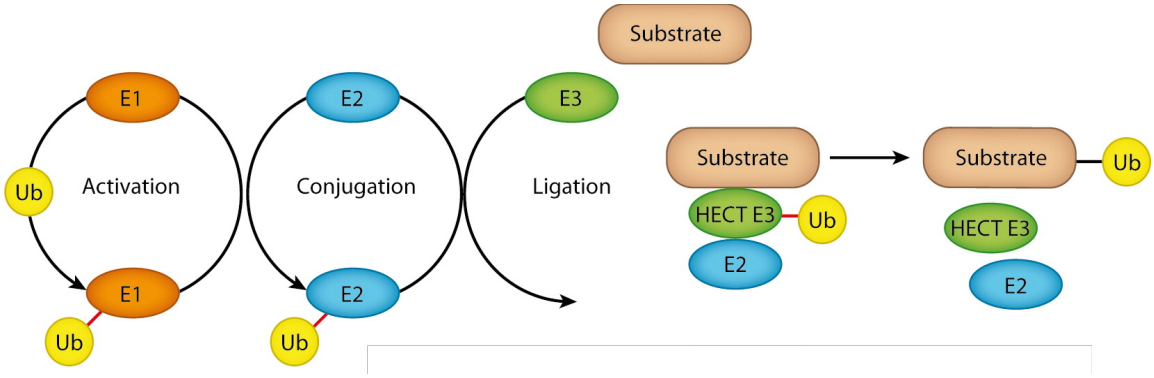

Figure 3. The three-step process of ubiquitination consisting of activation by an E1 enzyme, conjugation (E2 enzyme) and ligation (E3 or HECT E3 (E3 ubiquitin ligase containing the HECT domain)). An isopeptide bond is formed between ubiquitin and the substrate protein (Husnjak and Dikic, 2012).

Ubiquitin linkages primarily occur at the Lys48 residue, and these proteins are therefore marked for proteasomal degradation. Besides being marked for proteasomal degradation, ubiquitinated proteins can also be signals for various cellular processes. These usually include Lys63-linked poly-ubiquitin chains and are associated with cellular processes such as DNA repair and endocytosis (Aguilar and Wendland, 2003).

UCHL1 has also been associated with ubiquitin ligation. *In vitro* studies have demonstrated that UCHL1 has a ligase activity once it forms a homodimer. However, UCHL1 ligase function has not been demonstrated *in vivo*. It is unclear what regulates dimer formation and ligase activity but it is hypothesized it may be due to post-translational modifications or cytoplasmic events like membrane binding of a synaptic vesicle. Interestingly, UCHL1 ligase function is ATP independent, unlike other ubiquitin ligases that require ATP to activate ubiquitin (Liu *et al.,* 2002).

1.4 UCHL1 Interacting Proteins

1.4.1 UCHL1 and Ubiquitin

UCHL1 interacts with ubiquitin through its deubiquitinating and ubiquitinating activity. However, the first study to show UCHL1 activity *in vivo* demonstrated that UCHL1 has a role in ubiquitin homeostasis (Osaka *et al.,* 2003). UCHL1 was shown to interact and co-localize with ubiquitin. The interaction resulted in stabilization of mono-ubiquitin. Knockdown of UCHL1 resulted in decreased levels of ubiquitin while overexpression of UCHL1 resulted in increased levels of ubiquitin. UCHL1^{C90S}, which contains a mutated active site cysteine and lacks hydrolase activity, also interacts with ubiquitin and has a role in maintaining cellular levels of ubiquitin (Osaka *et al.,* 2003). This suggests that UCHL1 has a role in stability of ubiquitin rather than deubiquitination.

1.4.2 UCHL1 and p53

The transcription factor p53 plays a vital role in apoptosis but also in cell cycle regulation. It regulates many apoptotic and cell cycle genes resulting in downstream

pathways that lead to cell death. As a transcription factor, p53 binds to specific DNA sequences as a tetramer and regulates genes in a phosphorylation dependent manner. These include activation of genes such as *FAS, CDKN1A and BAX* (Pucci *et al.,* 2000). One such example is the activation of the Fas death receptor due to genotoxic stress. This was observed in leukemia T-cells in response to chemotherapy (Friesen *et al.,* 1996). p53 also directly activates the transcription of the *BAX* gene by binding to its promoter (Miyashita and Reed, 1995). Furthermore, p53 is also able to induce apoptosis through protein-protein interactions. This is the case with p53 and the DNA repair factor TFIIH (Transcription Factor II Human) (Wang *et al.,* 1996). Apart from its roles in apoptosis, p53 also plays a role in cell cycle arrest. In response to DNA damage, p53 activates the *CDKN1A* gene, which subsequently inhibits cyclin B-CDK4/6 and is unable to phosphorylate pRb (retinoblastoma protein). This results in cell cycle arrest at the G1/S checkpoint (Pucci *et al.,* 2000). Due to its wide range of roles in both inducing apoptosis or cell cycle arrest, p53 is often mutated and its function is lost in many cancer types.

UCHL1 has previously been shown to interact with p53. This was the case in UCHL1 overexpressed nasopharyngeal cancer cell lines and UCHL1 transfected HCT116 colorectal cancer cell line. UCHL1 and p53 also interact in HEK293T cells, where UCHL1 and p53 are endogenously expressed (Li *et al.,* 2010; Yu *et al.,* 2008). It is hypothesized that UCHL1 is a tumour suppressor protein that deubiquitinates p53 leading to its stabilization and activation resulting in apoptosis and cell cycle arrest. It is also proposed that the UCHL1 ligase function may play a role in the ubiquitination of the p53 negative regulator MDM2 (Li *et al.,* 2010). Additionally, the overexpression of UCHL1 in LNCaP prostate cancer cells leads to increased protein expression of p53 and $p14^{ARF}$

and decreased levels of the p53 negative regulator MDM2, suggesting that UCHL1 is a tumour suppressor that suppresses cell proliferation and anchorage-independent growth (Ummanni *et al.,* 2011).

1.4.3 UCHL1 and Cyclin-Dependent Kinases (CDKs)

A recent study by Kabuta *et al.,* 2013 showed that UCHL1 interacts with CDK1, CDK4, CDK5 and CDK6 enhancing the activity of the CDKs. The interaction between CDKs and UCHL1 is independent of UCHL1 DUB activity meaning UCHL1 does not deubiquitinate the CDKs in order to enhance their kinase activity. This was determined by mutating the active site cysteine generating $UCHL1^{C90S}$, which in fact still interacts with the four CDKs even without the DUB or ligase activity. It was also demonstrated that UCHL1 overexpression in HeLa cells, which do not express UCHL1, resulted in increase of cell proliferation. Similarly, UCHL1 knockdown in UCHL1 expressing cells resulted in decrease of cell proliferation (Kabuta *et al.,* 2013).

1.4.4 UCHL1 and the Shelterin Complex

A recent study by Lee *et al.,* 2011 has reported that UCHL1 interacts with two proteins of the shelterin complex, RAP1 and TIN2. In this study, the investigators identified over 300 proteins that are associated with at least one of the six core shelterin complex proteins (Lee *et al.,* 2011). The shelterin complex specifically binds to telomeric repeats.

1.4.4.1 Telomeric Repeats

Elizabeth Blackburn first discovered telomeres in 1978 (Blackburn and Gall, 1978). Telomeres are chromosome ends comprised of tandem telomeric repeats ($(TTAGGG)_n$) usually ranging from 5 to 15 kb in length (Sfeir, 2012). Telomeres also contain G-rich single-stranded overhangs that are 30 to 500 bases long (Chai *et al.,* 2004). These overhangs loop over to the double-stranded DNA and form a T-loop structure as well as displacement loop, D-loop (Figure 4). The shelterin protein complex plays a role in stabilizing the T-loop and protecting telomere ends (de Lange, 2005).

Telomeric repeats are not exclusive to only telomeric regions but are also within intrachromosomal sites (between telomeres and centromeres). These regions are known as interstitial telomeric sequences (ITSs). It is believed that these sites were generated through evolutionary chromosomal rearrangements such as chromosomal fusions and inversions. There are three types of ITSs and they include short ITSs (up to 20 telomeric repeat hexamers), long subtelomeric ITSs (several hundred base pairs of telomeric repeats) and fusion ITSs (telomeric repeats in a head-to-head orientation) (Azzalin *et al.,* 2001; Lin and Yan, 2008).

1.4.4.2 Shelterin Complex

The shelterin complex is comprised of six proteins that specifically bind to telomeric repeats. These proteins include telomeric repeat binding factors 1 and 2 (TRF1 and TRF2), TRF1-interacting nuclear factor 2 (TIN2), protector of telomeres protein 1 (POT1), POT1 and TIN2 interacting protein (TPP1) and repressor/activator protein 1 (RAP1) (Figure 4). The shelterin complex is essential in maintaining the integrity of

telomeres and preventing telomere dysfunction (de Lange, 2005; Sfeir, 2012). It has also been reported that the shelterin complex does not exclusively bind to only the telomeric regions but also to ITSs (Simonet *et al.,* 2011; Yang *et al.,* 2011).

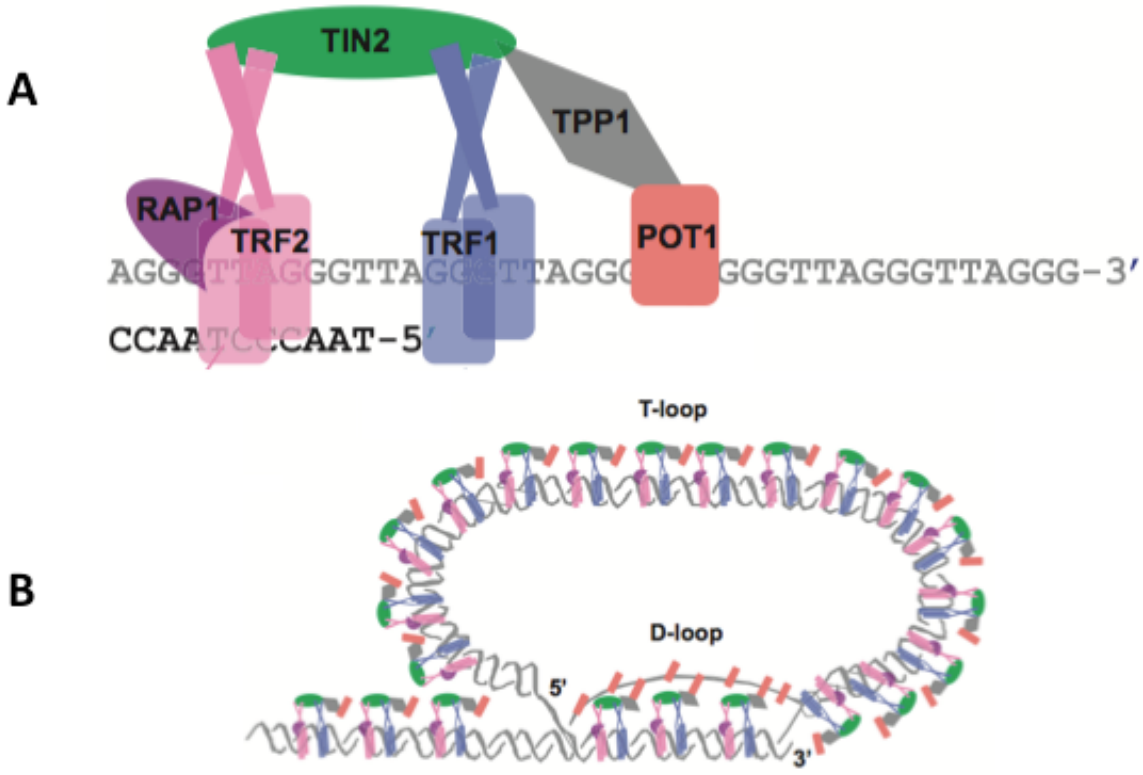

Figure 4. Schematic representation of the shelterin complex proteins TRF1, TRF2, RAP1, TIN2, TPP1 and POT1 binding to the telomere (A). The formation of the T- and D-loops (B) (Martinez and Blasco, 2010).

The first identified component of the shelterin complex was TRF1 (also known as TERF1). TRF1 consists of a C-terminal MYB domain, TRF homology (TRFH) domain and a N-terminal acidic domain. DNA binding of telomeric repeats by TRF1 is dimerization-dependent. Homodimerization occurs through the TRFH domains and subsequent DNA binding via the MYB domains of the two TRF1 proteins. The MYB domain recognizes and binds to 5'-YTA GGG TTR-3' (where Y represents a pyrimidine

base and R represents a purine) sequences of double-stranded DNA (de Lange, 2005; Diotti and Loayza, 2011; Martinez and Blasco, 2010). As part of the Shelterin complex TRF1 functions include the regulation of telomere length and protection of telomeres (de Lange, 2005).

Like TRF1, the TRF2 (also known as TERF2) protein also binds to double stranded 5'-YTA GGG TTR-3' DNA sequences via the MYB domain. TRF2 contains the TRFH domain and unlike TRF1, the N-terminal domain of TRF2 is basic and not acidic (Diotti and Loayza, 2011). Together, TRF2 and TRF1 inhibit the elongation of telomeres by the enzyme telomerase (Diotti and Loayza, 2011; van Steensel and de Lange, 1997). TRF2 also protects telomeres from being recognized by DNA repair machinery and undergoing non-homologous end joining (NHEJ). This would result in chromosome fusion (Sfeir, 2012). It is important to note that TRF2 expression is two-fold higher than that of TRF1. This is accounted by the fact that TRF2 forms other shelterin subcomplexes, which may have other roles independent of the TRF1 and TRF2 shelterin complexes (Diotti and Loayza, 2011; Liu *et al.,* 2004). TRF2 interacts with RAP1 (also known as telomeric repeat-binding factor 2-interacting protein 1 or TERF2IP). RAP1 has a role in telomere protection from NHEJ (Martinez and Blasco, 2010). It contains a MYB domain, a BRCT (BRCA1 C-terminal) motif and a TRF2 binding C-terminal domain. Interestingly, the human RAP1 does not bind telomeric DNA repeats directly despite the MYB domain, while yeast RAP1 is DNA binding (Hanaoka *et al.,* 2001).

The TIN2 (also known as TINF2) protein serves as a bridge between TRF1 and TRF2, allowing for an interaction between these two proteins. TIN2 is at the heart of the shelterin complex and also recruits TPP1 (also known as ACD and PIP1). TPP1

subsequently interacts with the sixth and final component of the shelterin complex, POT1. POT1 contains OB1 and OB2 domains thus having DNA binding capacity. Unlike TRF1 and TRF2, POT1 binds to 3'-single-stranded DNA repeat region of the G-overhang at the end of telomeres. POT1 stabilizes the T-loop and as part of the shelterin complex has a role in the protection of the telomere end (Xin *et al.,* 2008).

1.5 UCHL1 and Disease

1.5.1 UCHL1 and Neurodegenerative Disease

UCHL1 is the most widely studied UCH deubiquitinating enzyme in relation to neurodegenerative diseases. This is largely due to a point mutation that results in a mutant UCHL1 protein (I93M) and has been associated with Parkinson's disease, PARK5 (Leroy *et al.,* 1998). It was demonstrated that this missense mutation in a family with Parkinson's disease caused a substantial decrease in the deubiquitinating activity of UCHL1. Leroy *et al.,* 1998 have shown that this mutation results in a 50% decrease of catalytic activity and hypothesized that this results in subsequent aggregation of UCHL1 protein and UCHL1 substrates. However, this mutation has not been shown in any other Parkinson's disease cases and it remains to be seen if this is only an isolated case found in only this German family with Parkinson's disease. A separate study has reported that a S18Y single nucleotide polymorphism protects against Parkinson's disease. This UCHL1 variant is associated with lower risk of Parkinson's disease (Liu *et al.,* 2002). However, a subsequent study has questioned if UCHL1 is the susceptibility gene for Parkinson's disease and has not confirmed that the S18Y polymorphism is protective against the disease (Healy *et al.,* 2006).

The S18Y polymorphism has also been investigated in Alzheimer's disease. It has been reported that this UCHL1 polymorphism does not protect against Alzheimer's disease (Zetterberg *et al.,* 2010). Additionally, UCHL1 is downregulated in individuals with Alzheimer's disease as well as Parkinson's disease. It was also shown that UCHL1 is prone to oxidative damage and is associated with neurofibrillary tangles (Choi *et al.,* 2004). This suggests that UCHL1 is associated with the Alzheimer's and Parkinson's disease pathogenesis.

1.5.2 UCHL1 and Cancer

The specific role of UCHs in cancer is still largely unknown and remains an intriguing area of research. As is the case with neurodegenerative diseases, the most studied UCH associated with cancer is UCHL1. UCHL1 has been associated with a wide range of non-neuronal cancers. It is upregulated in breast cancer, lung adenocarcinoma, squamous cell carcinoma and colorectal cancer (Chen *et al.,* 2002; Ma *et al.,* 2010; Mastoraki *et al.,* 2009; Myoshi *et al.,* 2006). It is suggested that UCHL1 upregulation is associated with tumour aggressiveness and pathogenesis ultimately leading to poor prognosis (Akishima-Fukasawa *et al.,* 2010; Myoshi *et al.,* 2006; Tezel *et al.,* 2000). There have been multiple hypotheses how UCHL1 is implicated in oncogenesis. It was shown that UCHL1 interacts and stabilizes β-catenin leading to β-catenin regulated gene expression of potential oncogenes (Bheda *et al.,* 2009a). UCHL1 was also shown to be associated with JAB1 (Jun activation domain binding protein 1). This interaction leads to the translocation of the cell cycle progression regulator CDKN1B ($p27^{Kip1}$) to the cytoplasm, resulting in its proteasomal degradation (Caballero *et al.,* 2002). UCHL1

overexpression in benign prostate tumour cells led to epithelial-to-mesenchymal transition (EMT) and resulted in increased cancer cell invasion metastasis. Additionally, knockdown of UCHL1 in DU145 cells led to MET (opposite of EMT) and resulted in decreased cell invasiveness and migration (Jang *et al.,* 2011). UCHL1 knockdown results by Bheda *et al.,* 2009b have shown that UCHL1 controls the expression of pro- and anti-apoptotic genes as well as genes involved in cell cycle regulation. When UCHL1 was knocked down, pro-apoptotic and cell cycle arrest genes such as *BAX, BIK* and *CDKN1A* were upregulated while anti-apoptotic genes such as *MYC* and *RHOA* were downregulated leading to the conclusion that UCHL1 is an oncogene (Bheda *et al.,* 2009b). The mechanism how UCHL1 regulates the expression of these genes is unknown.

On the other hand, it has also been reported that UCHL1 expression is supressed in several cancers due to the hypermethylation of the *UCHL1* upstream promoter thus labelling UCHL1 as a potential tumour suppressor. This was the case in prostate, nasopharyngeal and breast cancer (Li *et al.,* 2010; Tokumaru *et al.,* 2008; Ummanni *et al.,* 2011). Treatment of cancer cells with DNA methyltransferase inhibitor 5-aza-2′-deoxycytidine resulted in induction of *UCHL1* expression (Mitsui *et al.,* 2012; Tokumaru *et al.,* 2008). Mitsui *et al.,* 2012 suggest that UCHL1 promoter methylation can be used as a marker for biochemical recurrence in prostate cancer after radical prostatectomy. It is disputed whether UCHL1 has oncogenic or tumour suppressor ability and what is the mechanism of the UCHL1 function in cancer. UCHL1 has been shown to interact with tumour suppressor p53 when expressed in cancer cells. This led to the hypothesis that

UCHL1 deubiquitinates and stabilizes p53 leading to apoptosis and cell cycle arrest (Li *et al.,* 2010).

1.6 Epigenetics and UCHL1

1.6.1 Epigenetics

Epigenetics is defined as the study of heritable changes in phenotype or gene expression without alterations in the DNA sequence (Delcuve *et al.,* 2009; Tsai and Baylin, 2011). These include posttranslational modifications (PTMs) that modify chromatin and in turn play an important role in gene expression. These modifications include DNA methylation as well as modifications such as histone acetylation, methylation, phosphorylation or ubiquitination.

DNA methylation is the addition of a methyl group (CH_3) to the 5' position of cytosine nucleotides of CpG islands by DNA methyltransferases (DNMT). This process plays a vital role in gene silencing, as approximately 50% of CpG islands are located in promoter (regulatory) regions of genes (Siedlecki and Zielenkiewicz, 2006). DNA methylation plays a role in gene suppression by being a marker for methyl CpG-binding domain (MBD) proteins, which subsequently recruit histone deacetylases and other chromatin remodelling complexes. In cancer, certain genes such as tumour suppressors or DNA repair genes like *MLH1* can be silenced by DNA methylation (Tsai and Baylin, 2011).

PTMs of histones are markers for subsequent recruitment of protein complexes that control gene expression. These include PTMs of core histones H2A, H2B, H3 and H4 as well as various histone variants. Histone modifications can be both a

transcriptional activation and repression marker. For example, methylation of histone H3 at Lys4 (K4) results in transcriptional activation, while H3K9 methylation is a marker for heterochromatin and transcriptional suppression. It is also important to note that a single lysine residue can be methylated multiple times resulting in mono-, di- or trimethylation and thus resulting in different transcriptional markers (Kouzarides, 2007). As is the case with methylation, lysine residues of histones are crucial for acetylation (addition of $COCH_3$) by lysine acetyltransferases (KATs). The most notable acetylation mark is H3K9, which results in transcriptional activation. Interestingly, phosphorylation (addition of PO_4^{3-}) of H3S10 results in transcriptional activation as well as the in the condensation of mitotic chromosomes meaning chromatin opens and closes in each case, respectively (Berger, 2007). The addition of proteins like SUMO and ubiquitin to histones H2A and H2B also results in different transcriptional markers. SUMOylation of histones H2A, H2B and H4 is associated with transcriptional repression (Berger, 2007; Shiio and Eisenman, 2003). Ubiquitination of histone H2A also results in transcriptional repression while ubiquitination of histone H2B results in activation. Histone H2A and H2B ubiquitination is also reversible by DUBs. Therefore, histone H2A deubiquitination by DUBs like USP16 or USP21 leads to transcriptional activation. On the other hand, deubiquitination of histone H2B primarily leads to transcriptional activation (Cao and Yan, 2012). Similarly, all histone PTMs are also reversible by proteins such as demethylases, histone deacetylases (HDACs) or phosphatases (Berger, 2007). Histone modifications can have a direct effect on gene expression by altering the chromatin structure but also indirect by recruiting protein complexes such as chromatin modifying proteins.

1.6.2 UCHL1 and Epigenetics

As previously stated, it has been suggested that UCHL1 expression is silenced in several cancers due to the hypermethylation of the *UCHL1* upstream promoter. This includes prostate, nasopharyngeal and breast cancers (Li *et al.,* 2010; Tokumaru *et al.,* 2008; Ummanni *et al.,* 2011). Due to this reason, it has been proposed that UCHL1 is a tumour suppressor gene. Several studies have shown that treatment of cancer cells that do not express UCHL1 with the DNA methyltransferase 1 inhibitor, 5-aza-2′-deoxycytidine, induces the expression of UCHL1 mRNA. However, induction of UCHL1 with 5-aza-2′-deoxycytidine is in some cases inconsistent. For example, Mitsui *et al.,* 2012 were able to induce UCHL1 mRNA expression in both LNCaP and PC3 prostate cancer cells whereas Tokumaru *et al.,* 2008 induced very little UCHL1 mRNA expression in LNCaP but not in PC3 prostate cancer cells.

1.7 Prostate Cancer

1.7.1 Prostate Cancer

Prostate cancer is the second most diagnosed cancer in males worldwide and the sixth leading cause of cancer death. Developed countries of North America, Europe and Oceania have the highest incidence of prostate cancer, where it is the most commonly diagnosed and the third leading cause of cancer death in males (Jemal *et al.,* 2011). This also applies to Canada and according to Canadian Cancer Statistics, it is the most diagnosed cancer (23,600 cases) and the third leading cause of death (3,900) in males in 2013. Prostate cancer is a disease of the elderly where most men will develop prostate

cancer by the latter stages of life and many might die of other causes without ever being diagnosed.

Prostate cancer is a very heterogeneous disease. This is explained by numerous genetic variations such as ploidy, chromosomal alterations, gene expression, ethnic or geographic heterogeneity as well as androgen receptor (AR) expression (Boyd *et al.,* 2012). In early stages, prostate cancer cells are androgen-dependent (AD) meaning they require androgen for growth. Further development leads to some cells becoming androgen-sensitive (AS), where they do not require androgen for growth but still respond to androgen. A treatment for AD and AS prostate cancer is initially hormone therapy (androgen-deprivation therapy) (Abrahamsson, 2009). Even though this may lead to remission of the disease, it can also cause alterations in the AR and the cells no longer need androgen for growth thus the disease becomes androgen-independent (AI) (Laufer *et al.,* 2000). AI is also referred to castration-resistant prostate cancer (CRPC) (Seruga *et al.,* 2011). The AR can become mutated or even completely lost in the cancer cells (Culig *et al.,* 1998; Kinoshita *et al.,* 2000). Prostate cancer cells express the prostate-specific antigen (PSA) that is used as a marker for diagnosis of metastatic prostate cancer in other tissues (Balk *et al.,* 2003; Polascik *et al.,* 1999). Prostate cancer tends to primarily metastasize to the lymph nodes and bone but also to other organs.

1.7.2 Prostate Cancer Model Cell Lines

The most widely used prostate cancer cell lines in research are LNCaP and PC3. During this study, LNCaP and PC3 cell lines were used, along with DU145 and C4-2 prostate cancer cell lines. The LNCaP prostate cancer cell line was derived from a lymph

node metastasis site of a 50-year-old male (Horoszericz *et al.,* 1980). It is AR positive and AS. The PC3 prostate cancer cell line was derived from a bone (lumbar) metastasis site of a 62-year-old male (Kaighn *et al.,* 1979). It is AR negative and AI. The DU145 prostate cancer cell line was derived from a central nervous system metastasis site of a 69-year-old male (Stone *et al.,* 1978). Like PC3, it is also AR negative and AI. The C4-2 prostate cancer cell line is a subline of LNCaP obtained through co-injection of LNCaP cells and human bone MS fibroblasts (derived from bone osteosarcoma) into mice. The mice were subsequently castrated and the C4 (castrated after 4 weeks) tumour cell line was derived. The second co-injection of C4 cells and human bone MS fibroblasts into castrated mice resulted in collection of the C4-2 cells (Thalmann *et al.,* 1994). These cells are castration-resistant (AI) but retain the AR making it a suitable model cell line since the AR is typically retained in prostate tumours.

1.8 Chromatin Immunoprecipitation (ChIP) and Next-Generation Sequencing (NGS)

1.8.1 Chromatin Immunoprecipitation (ChIP)

Chromatin immunoprecipitation (ChIP) is an assay used to study the interaction between DNA and proteins. As its name suggests, it is an immunoprecipitation technique where the protein of interest is immunoprecipitated along with the interacting DNA, allowing for downstream study of the DNA sequences associated with the protein. The ChIP assay can be utilized to study and map the localization of DNA associated proteins such as modified histones, transcription factors or chromatin modifying enzymes. The ChIP assay was developed by Gilmour and Lis is 1984. ChIP was utilized to study RNA polymerase II in Drosophila (Gilmour and Lis, 1985). There are two kinds of the ChIP

assays, cross-linked ChIP (X-ChIP) and native ChIP (N-ChIP). The X-ChIP assay uses cross-linking to fix the protein and DNA interaction, while N-ChIP is done under native conditions and there is no cross-linking step. During this study, X-ChIP was performed to study the association of UCHL1 with DNA.

ChIP is quite a lengthy method that initially requires thorough optimization steps (for more details refer to Section 3.4). Briefly, the protocol can be divided into five major steps. The first step is the cross-linking of cells to keep the protein and DNA interaction intact. The protocol can also be modified to include a protein-to-protein cross-linking step in case the protein of interest is associated with DNA indirectly. The second step is the lysing of the cellular membrane to obtain nuclei, lysing of the nuclei and fragmentation of DNA. The DNA can be fragmented by sonication (shearing) or by micrococcal nuclease (MNase) digestion. This is followed by the third step, which is antibody immunoprecipitation of the protein of interest. The fourth step is the washing of the immunoprecipitated fraction followed by elution and the reversal of protein and DNA cross-linking. The fifth and final step is the purification of the ChIP DNA and the downstream applications such as PCR or ChIP-seq by next-generation sequencing (NGS).

1.8.2 Next-Generation Sequencing (NGS)

For several decades Sanger (chain-termination) sequencing was the most commonly used method for DNA sequencing. In recent years, major strides have been made to produce cost effective sequencing methods and at the same time being able to sequence millions of reads in parallel. Since 2005, NGS has become a widely used

method that is able to sequence the human genome in a span of just a few weeks costing approximately $5,000 (Mardis, 2013). Multiple NGS technologies have been developed and enhanced over the recent years including Roche 454 FXL, Illumina HiSeq 2000 and Life Technologies SOLiD sequencer.

1.8.2.1 The SOLiD Sequencing Platform

During this study, the SOLiD (Sequencing by Oligo Ligation and Detection) sequencing platform was used. SOLiD sequencing was developed by Applied Biosystems and later acquired by Life Technologies. It is referred to as a two-base sequencing ligation based method (Liu *et al.,* 2012).

Before sequencing the specific DNA fragments, adaptors are first ligated to the ends of the fragments. This is followed by emulsion PCR (ePCR) where the adaptor-DNA linked oligonucleotides bind to complementary adaptors that are attached to beads. The DNA is then amplified and the beads are attached to a glass slide and placed into the sequencer (Mardis, 2008a). SOLiD sequencing is ligation based and is initiated by annealing of a primer to the adaptor sequence (Figure 5). Semi-degenerative 8-mer oligonucleotides are added. Starting at the 3' end, these oligonucleotides contain complementary bases at positions 1 and 2, degenerate bases 3-5, a cleavage site between 5 and 6, degenerate bases 6-8 (subsequently cleaved off) and a fluorescent group at position 8 (5' end) (Mardis, 2008a). When a specific 8-mer matches to the DNA sequence, it hybridizes adjacent to the 3' end of the primer and is ligated. The fluorescence is measured and bases 6-8 are cleaved off along with the fluorescent group allowing for further ligation rounds. Once the additional cycles yield a specific read

length, the newly synthesized fragment is removed and the second round of ligation starts at the n-1 position ('primer reset'; one base shift from where the primer in round one annealed to). There are three additional ligation rounds (five in total) and in each case there is a one base shift compared to the preceding round (Mardis, 2008a; Mardis, 2008b). SOLiD sequencing is a two-base encoding method that allows for better accuracy and distinguishing between true SNPs and sequencing errors.

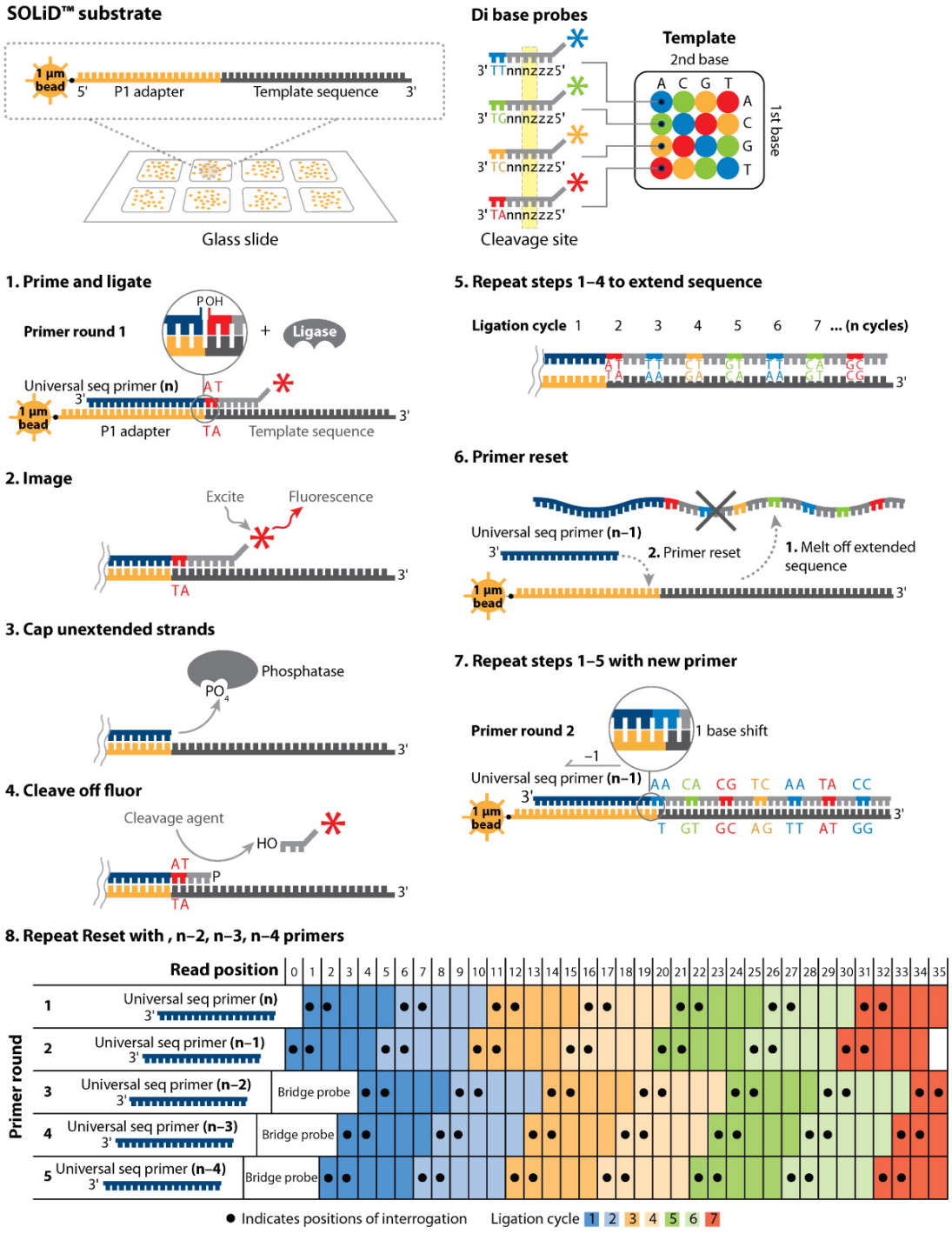

Figure 5. Overview of the sequencing steps by the SOLiD platform. A matching 8-mer hybridizes adjacent to the 3' end of the primer and is ligated (1). The fluorescence is measured and bases 6-8 are cleaved off along with the fluorescent group (2-4). Additional cycles then yield a specific read length (5). The newly synthesized fragment is removed and the second round of ligation starts at the n-1 position (6-7). There are three additional ligation rounds (five in total) and in each case there is a one base shift compared to the preceding round (8) (Mardis, 2008b).

1.8.3 ChIP-Sequencing (ChIP-seq)

ChIP-seq is an unbiased screening approach that allows for whole genome mapping of a protein's binding sites to DNA. Through NGS it is possible to sequence the immunoprecipitated DNA associated with the protein of interest. It is important to obtain approximately 20 ng of ChIP DNA for sequencing with the SOLiD platform. DNA fragment ends are then repaired followed by the adaptor ligation. Subsequently, the DNA is amplified by ePCR generating a ChIP-seq library that is sequenced by the SOLiD sequencer. After sequencing is finished, the raw data is analyzed and mapped to the human reference genome (hg19). This allows for mapping of ChIP-seq peaks and identifying locations of the target (binding) sites of the protein of interest.

Chapter 2: Rationale, Hypothesis and Project Aims

2.1 Rationale

UCHL1 is primarily expressed in neuronal cells, the pancreas (islets of Langerhans) and neuroendocrine cells (Day and Thompson, 2010). It is multifunctional protein involved in numerous cellular processes including deubiquitination, ubiquitination, ubiquitin homeostasis and enhancing CDK activity. UCHL1 has been linked with neurodegenerative diseases and a wide range of cancers but its specific role remains unknown. To date, UCHL1 association with DNA has never been reported. Preliminary data from the Davie lab indicates that UCHL1 is differentially cross-linked to DNA in DU145 (AR negative and AI; derived from a central nervous system metastasis site) prostate cancer cells and not in BPH1 (benign prostate hyperplasia; non tumorigenic), PC3 (AR negative and AI; derived from a bone (lumbar) metastasis site) and LNCaP (AR positive and AS; derived from a lymph node metastasis site) cells. It has also been confirmed by immunoblot analyses that UCHL1 is only expressed in DU145 and not in BPH1, LNCaP, PC3 or C4-2 (LNCaP subline) prostate cancer cells. It has been suggested that UCHL1 expression is silenced in several cancers due to the hypermethylation of the *UCHL1* upstream promoter. This includes prostate, nasopharyngeal and breast cancers (Li *et al.,* 2010; Tokumaru *et al.,* 2008; Ummanni *et al.,* 2011). Treatment of cancer cells that do not express UCHL1 with epigenetic drugs will determine if UCHL1 expression can be induced in these prostate cancer cells and whether the induction will re-instate UCHL1 association with genomic DNA.

The Davie lab has previously applied a successful approach in discovering proteins that do not have a known association with DNA but can be cross-linked to DNA in cancer cells. This was the case with peroxiredoxin 1 (PRDX1) being cross-linked to DNA, along with its interacting partner NF-κB, on the NF-κB binding sites of the upstream promoter region of the cyclooxygenase-2 (*COX2 or PRGS2*) gene in ER- breast cancer cells (Wang *et al.,* 2010). Since there are reports of UCHL1 interacting with the transcription factor p53, it was investigated whether UCHL1 is recruited to the genome via a transcription factor, i.e., whether p53 recruits UCHL1 to genomic sites binding p53. UCHL1 knockdown studies by Bheda *et al.,* 2009b have shown that UCHL1 controls the expression of pro- and anti-apoptotic genes as well as genes involved in cell cycle regulation in HEK293T (human embryonic kidney cells that contain the Simian virus 40 (SV40) large T antigen), KR4 (Epstein-Barr virus transformed B-cells) and C33A (cervical cancer cells) cells. It is important to note that HEK293T are UCHL1 expressing cells that are possibly of neuronal origin as these cells express many neuronal markers (Shaw *et al.,* 2002). The mechanism how UCHL1 controls the expression of pro- and anti-apoptotic as well as cell cycle regulation genes still remains unknown. Furthermore, UCHL1 could be associated with other DNA-binding proteins and ChIP-seq analyses will identify potential UCHL1 DNA binding sites in DU145 and HEK293T cells.

2.2 Hypothesis

UCHL1 regulates the expression of pro- or anti-apoptotic genes as well as the expression of genes involved in the cell cycle through its interaction with DNA (either directly or indirectly).

2.3 Specific Aims

2.3.1 Aim 1: To Determine Whether Induced UCHL1 Expression in LNCaP, C4-2 and PC3 Cells Re-Instates Association with Genomic DNA

UCHL1 is not expressed in PC3, LNCaP and C4-2 prostate cancer cell lines. Previous studies have demonstrated that treatment of the LNCaP and PC3 prostate cancer cells with the DNA methyltransferase 1 inhibitor, 5-aza-2′-deoxycytidine, induces the expression of UCHL1 mRNA (Mitsui *et al.,* 2012; Tokumaru *et al.,* 2008). Since C4-2 is a subline of LNCaP, it was also expected that UCHL1 would be expressed after treatment. LNCaP, C4-2 and PC-3 cells were treated with 5-aza-2′-deoxycytidine. If 5-aza-2′-deoxycytidine alone does not result in UCHL1 expression, the cells would be treated with a histone deacetylase inhibitor such as trichostatin A (TSA) together with 5-aza-2′-deoxycytidine. RT-PCR and immunoblot analyses would determine if UCHL1 is expressed in treated cells. If UCHL1 is induced, the PC3, LNCaP and C4-2 cells treated with epigenetic drugs would be cross-linked with formaldehyde to determine if the induced UCHL1 protein is bound to genomic DNA.

2.3.2 Aim 2

2.3.2.1 Aim 2 – A: To Determine Whether UCHL1 Interacts with the p53 Transcription Factor in the DU145 Prostate Cancer Cell Line and Whether UCHL1 Co-Localizes with p53 on the Promoter Regions of *CDKN1A* and *BAX* Genes in DU145 Prostate Cancer Cell Line

Previous studies have demonstrated that UCHL1 interacts with p53 in UCHL1 overexpressed nasopharyngeal cancer cell lines, transfected HCT116 colorectal cancer cell line and HEK293T cells, where UCHL1 and p53 are endogenously expressed (Li *et al.,* 2010; Yu *et al.,* 2008). Co-immunoprecipitation (Co-IP) and immunoblot analyses

will determine whether UCHL1 interacts with p53 in DU145 cells. Li et al., 2010 have performed a p53 IP and UCHL1 immunoblot showing there is an interaction between the proteins but the authors never performed the reciprocal IP. If these two proteins were associated, then the candidate approach would be applied to determine if UCHL1 is co-associated with p53 at p53 genomic binding sites.

UCHL1 was cross-linked to DNA with formaldehyde or cisplatin in DU145 but not in BPH1, PC3 or LNCaP cells. Also, it was unknown if UCHL1 was cross-linked to DNA in HEK293T cells and by determining this it would be possible to further study this interaction in this particular cell line. Bheda et al., 2009b have shown that UCHL1 controls the expression of pro- and anti-apoptotic genes as well as genes involved in cell cycle regulation in HEK293T cells. The application of the ChIP assay would be able to identify the DNA sequences associated with UCHL1 and whether UCHL1 and p53 co-localize to the same genomic regions. Two genes regulated by p53 were chosen for this study, *CDKN1A* and *BAX*. *CDKN1A* codes for the cell cycle regulator $p21^{Waf1}$ while *BAX* codes for a pro-apoptotic BCL2 family member (Beckerman and Prives, 2010). In case UCHL1 is recruited to DNA by a transcription factor, dual cross-linking would also be performed with both dithiobis[succinimidyl propionate] (DSP) and formaldehyde to cross-link UCHL1 to the transcription factor and then cross-link the complex to DNA. The ChIP DNA would be isolated and interrogated with primers placed on either side of known p53 DNA binding sites.

2.3.2.2 Aim 2 – B: To Determine the Genomic Distribution of UCHL1 in DU145 Prostate Cancer Cells and HEK293T Cells by ChIP-Sequencing

If UCHL1 is found localized in the regulatory regions of genes, this would suggest that it has a role in the regulation of gene expression. Since the locations where UCHL1 interacts with DNA are unknown and there are no potential targets, ChIP-seq is an excellent method to identify potential UCHL1 DNA binding sites and shed light on a possible role of UCHL1. ChIP sequencing (ChIP-seq) is an unbiased screening approach that would be applied to determine the genomic location of UCHL1. The SOLiD System 5500xl Next Generation Sequencer was used during this study. The sequencing data would most likely identify many loci to which these proteins are bound as well as what region of genomic DNA UCHL1 are associated with, whether it is the promoter, coding or non-coding regions. It is possible that UCHL1 is recruited to the DNA by other transcription factors and *in silico* analyses would determine other possible transcription factor binding sites on the ChIP DNA. If UCHL1 is recruited to DNA by a transcription factor, dual cross-linking of DU145 and HEK293T cells would also be performed with both DSP and formaldehyde to cross-link UCHL1 to the transcription factor and then cross-link the complex to DNA. UCHL1 knockdown results by Bheda et al., 2009b have shown that UCHL1 controls the expression of pro- and anti-apoptotic genes as well as genes involved in cell cycle regulation. ChIP-seq analyses would be able to determine if UCHL1 plays a role in gene expression of these genes in this particular cell line. The data analyses (mapping and mining) would be performed with the help of bioinformatician Dr Wayne Xu. The UCHL1 targets on the genomic DNA would be validated by qPCR by using primers of the protein binding sites of interest.

Chapter 3: Materials and Methods

3.1 Cell Culture

3.1.1 Cell Culture Conditions

Cells lines LNCaP, PC3, BPH1, DU145 and HEK293T were obtained from the American Type Culture Collection (ATCC). The C4-2 cell line was obtained from Dr Paul Rennie at the Vancouver Prostate Centre. The human prostate cancer cell lines LNCaP, PC3 and C4-2 as well as the BPH1 cells were grown in RPMI-1640 media (Invitrogen). The DU145 prostate cancer cells were grown in EMEM media (Invitrogen). HEK293T cells were grown in DMEM media (Invitrogen). All of the media were supplemented with 10% FBS and 1% antibiotic-antimycotic (Invitrogen). The cells were grown at 37°C containing 5% CO_2.

3.1.2 Cell Passaging

The cells were passaged once reaching a confluency of 60-80%. First, the media was aspirated from the cell culture plate and the cell layer was washed with 1xPBS. This was followed by addition of 1-2 mL of TripLE Express trypsin (Gibco) and incubation at 37°C for 2-5 minutes, depending on the cell line. The detached cells were collected in appropriate media and transferred into a 15 mL centrifuge tube (VWR). The cells were centrifuged at 300xg for 3 minutes. The supernatant was aspirated and the cell pellet was resuspended in an appropriate volume of media. The resuspended cells were then seeded to new culture plates depending on the cell line and required amount of cells for experimental analyses.

3.1.3 Cell Storage and Recovery

Cells (80-90% confluent) were washed with 1xPBS followed by addition of 1-2 mL of TripLE Express trypsin (Gibco). The detached cells were collected in appropriate media, centrifuged at 300xg for 3 minutes and the supernatant was aspirated. The cell pellet was resuspended in FBS (Gibco) and DMSO (Sigma), 90% v/v FBS and 10% v/v DMSO. The resuspended cells were transferred to cryovials (Fisher Scientific), which were placed into an -80°C freezer. For long-term storage, the cryovials were then transferred to a liquid nitrogen tank.

The frozen cells were recovered by placing the cryovials in a 37°C water bath. Once thawed, the cells were transferred to a 15 mL centrifuge tube (VWR), which contained approximately 10 mL of appropriate media for the specific cell line. The cells were centrifuged at 300xg for 3 minutes. The supernatant (media, FBS and DMSO) was aspirated, the cell pellet was resuspended in 5 mL of media and the cells were transferred to a 5 cm culture plate. The media was changed after 24 hours or if 60-80% confluent, the cells were passaged and transferred to 10 or 15 cm culture plates. Before the cells were used for experimental analyses, they were passaged a minimum of three times.

3.2 Protein-Based Techniques

3.2.1 Preparation of Total Cellular Lysate

Cells (80-90% confluent) were washed two times with cold 1xPBS and harvested in 1xPBS from cell culture plates into 15 mL tubes. The cell pellet was obtained by centrifugation for 3 minutes at 300xg. The 1xPBS was aspirated and the cell pellet was resuspended in cold lysis buffer (50 mM Tris-HCl pH 8, 150 mM NaCl, 1 mM EDTA

and 0.5% NP-40), containing protease and phosphatase inhibitors (Roche), followed by incubation on ice for approximately 20 minutes. It was then sonicated three times for 3-5 seconds each time, with 30-second intervals on ice between sonication cycles. The cell lysate was centrifuged for 10 minutes at 17 000xg at 4°C and the supernatant was kept while the insoluble fraction was discarded. The protein concentration of the total cellular lysate (supernatant) was quantified according to the manufacturer's instructions using the Coomassie Plus Protein Assay Reagent (Fisher Scientific) and BSA as a standard. Once quantified, the total cellular lysates were stored at -20°C or -80°C.

3.2.2 SDS-PAGE and Western Blotting

Protein samples were reduced and denatured by the addition of the reducing sodium dodecyl sulfate (SDS) loading buffer (62.5 mM Tris-HCl pH 6.8, 25% glycerol, 2% SDS, 0.01% bromophenol blue and 5% β-mercapthoethanol) and boiled for approximately 5 minutes before being loaded onto a polyacrylamide gel. The polyacrylamide gel percentage (10%, 12% or 15%) was chosen depending on the size of the target protein. SDS-PAGE was started at 80V for approximately 20-30 minutes until the samples have entered the separating gel. The voltage was then increased to 100V or 120V for an additional 1-1.5 hour. Using the wet transfer apparatus (Biorad), the proteins were transferred from the polyacrylamide gel to a 0.45 μm nitrocellulose membrane (Biorad) at 100V for 1 hour at 4°C. To test the efficacy of the transfer, the membrane was stained with Ponceau S (0.5% Ponceau S and 5% acetic acid) for 2-3 minutes. The stained membrane was washed with ddH_2O for 5-10 minutes and then baked at 65°C for 20-30 minutes. The baked membrane was blocked with 5% (w/v) skim milk powder in

0.1% TBST (50 mM Tris-HCl pH 7.6, 150 mM NaCl and 0.1% Tween-20) at room temperature for 1 hour on a rocking platform (VWR, Model 200). After blocking, the membrane was incubated with a primary antibody at an optimized dilution in 5% skim milk in 0.1% TBST. The primary antibody incubation was usually done overnight at 4°C on a rotator (Boekel Scientific, Model 260200). Alternatively, the primary antibody incubation can also be performed for 1 hour at room temperature. The membrane was then washed three times (10 minutes per wash) at room temperature with 0.1% TBST on the rocking platform. The membrane was then incubated for 1 hour at room temperature with the appropriate horseradish peroxidase-conjugated anti-IgG secondary antibody diluted in 5% skim milk. After secondary antibody incubation, the membrane was washed three times (10 minutes per wash) at room temperature with 0.1% TBST on the rocking platform. Lastly, the target protein on the membrane was visualized with Western Lighting Plus-ECL (Perkin Elmer) on Hyperfilm ECL (Amersham) in accordance with manufacturers' instructions.

3.3 DNA-Based Techniques

3.3.1 DNA Purification

ChIP DNA and PCR product DNA was purified by using the QIAquick PCR Purification Kit according to the manufacturer's instructions (Qiagen). The DNA was eluted with 40 μL of nuclease free water (Fisher). The DNA was then used for qPCR, agarose gel or bioanalyzer analyses.

3.3.2 Agarose Gels

Agarose gels with concentrations from 0.8% to 1.5% were generally prepared. The appropriate weight of agarose (Invitrogen) was dissolved in 1xTBE buffer (100 mM Tris base, 100 mM boric acid and 2 mM EDTA) and heated in the microwave for 1-2 minutes. The heated agarose was left to cool and 1xGelStar nucleic acid stain (Lonza) was added to the liquid agarose. The agarose gel was cast and left to solidify. The 1xTBE buffer was used for agarose gel electrophoresis.

3.4 Isolation and Analysis of Proteins Cross-Linked to DNA

Sumin Lu performed the initial analyses of DNA cross-linked proteins by cisplatin cross-linking. In brief, the BPH1, DU145, LNCaP and PC3 cell lines were incubated with cisplatin, lysed and applied to hydroxyapatite. After washes of the hydroxyapatite, thiourea was then used to reverse the cross-linking separating the protein from hydroxyapatite bound DNA followed by two-dimensional (2D) gel electrophoresis. The 2D gels were silver stained and the gel patterns were imaged using the Molecular Imager Fx (Bio-Rad) and analyzed with the PDQuest™ 2-D Analysis Software. The 2D gel patterns allow for analysis of differentially bound proteins to DNA cell lines, where the proteins of interest were cut out from the 2D gel and identified by mass spectrometry.

The subsequent analyses of DNA cross-linked proteins were performed by using formaldehyde instead of cisplatin. The DU145 and HEK293T cells were cross-linked with formaldehyde only (1%; 10 minutes at room temperature) or a combination of DSP (1 mM; 30 minutes at room temperature) and formaldehyde (0.5% or 1%; 10 minutes at room temperature). The cross-linking was stopped by the addition of 1.25 M glycine to a

final concentration of 125 mM and incubated for 5 minutes. The cross-linked cells were washed with 1xPBS and centrifuged at 300xg for 3 minutes. The cell pellets were either stored at -80°C or used immediately for isolation of proteins cross-linked to DNA. The cell pellets (generally four 150 mm cell plates per cell line or cross-linking condition) were resuspended in cold lysis buffer (5 M urea, 2 M guanidine hydrochloride, 2 M NaCl and 0.2 M potassium phosphate buffer, pH 7.5) with 1 mM PMSF (Sigma). The cells were sonicated on ice two times for 30 seconds at setting 3. The sonicated supernatant was centrifuged at 3345xg for 10 minutes. The supernatant was retained and the pellet was discarded. The A_{260} reading of the supernatant was measured by Ultrospec 3000 UV/Visible Spectrophotometer (Pharmacia Biotech). Equal A_{260} concentrations were used for each cell line or cross-linking condition. Equal weight of hydroxyapatite (Bio-rad) was measured according to the A_{260} concentration (1 g of hydroxyapatite per 80 A_{260}). The hydroxyapatite was rehydrated in 50 mL centrifuge tubes on ice by adding 15-30 mL of lysis buffer and setting it on ice for 20 minutes. The lysis buffer was discarded, the sonicated lysate was added to the hydroxyapatite pellet and incubated for 1 hour at 4°C on a rotator. The lysate and hydroxyapatite tube was then centrifuged at 3345xg for 10 minutes and the supernatant was discarded. The hydroxyapatite pellet was then washed 5 times with 15-20 mL of lysis buffer with 1 mM PMSF, each time rotated until fully resuspended and centrifuged at 3345xg for 5 minutes. The washed hydroxyapatite pellet was resuspended in 10 mL of lysis buffer with 1 mM PMSF and incubated in a 65°C water bath overnight to reverse the DNA-protein cross-links. The hydroxyapatite was pelleted the following day by centrifugation at 3345xg for 10 minutes. The supernatant containing DNA cross-linked proteins was transferred to a fresh tube 15 mL

centrifuge tube and kept on ice. The supernatant was transferred to dialysis bags, placed into 2 L plastic beaker and dialyzed against 4 changes of water at 4°C for 27-30 hours. The dialyzed supernatant was transferred to a fresh tube 15 mL centrifuge tube and allowed to freeze down to -80°C overnight. The frozen supernatant was lyophilized overnight to obtain a concentrated protein pellet. Depending on size, the pellet was resuspended in 40-100 µL of water. The protein concentration was quantified according to the manufacturer's instructions using the Coomassie Plus Protein Assay Reagent (Fisher Scientific) and BSA as a standard. This was followed by SDS-PAGE and western blot analyses.

3.5 Chromatin Immunoprecipitation (ChIP) and ChIP-Sequencing (ChIP-seq)

3.5.1 ChIP

As described in Section 3.4, the DU145 and HEK293T cells were cross-linked with formaldehyde only or with a combination of DSP and formaldehyde. The cell pellet was resuspended in cell lysis buffer (5 mM PIPES pH 8, 85 mM KCl and 0.5% NP-40) supplemented with protease and phosphatase inhibitors. The cells were incubated for 10 minutes at 4°C with rotation followed by centrifugation at 2000xg for 5 minutes. The cell lysis step and centrifugation was repeated one more time to obtain nuclei. The nuclear pellet was resuspended in 1-2 mL of MNase digestion buffer (10 mM Tris-HCl pH 7.5, 0.25 M sucrose and 75 mM NaCl) supplemented with protease and phosphatase inhibitors. The DNA was then fragmented by sonication or MNase enzyme digestion (Figure 6).

When the DNA was fragmented by sonication, SDS to a final concentration of 0.3% was added to the resuspended nuclear pellet in MNase digestion buffer (sonication buffer) and incubated at room temperature 1-2 hours with rotation. The DNA was sonicated generally for 30-40 cycles of 5 seconds each at setting 3. The sonicated nuclear lysate was centrifuged for 10 minutes at 17 000xg at 4°C and the supernatant was diluted 5 fold with RIPA buffer (10 mM Tris-HCl pH 8, 1% Triton-X-100, 0.1% SDS and 0.1% SDC) supplemented with protease and phosphatase inhibitors.

When the DNA was fragmented by MNase digestion, the A_{260} reading of the resuspended nuclei was first measured and $CaCl_2$ to a final concentration of 3 mM was added. The sample was warmed in a water bath at 37°C for 10 minutes. Then, MNase (Worthington Biochemical Corporation) was added at a concentration of 2.5 U per 1 A_{260} and incubated at 37°C for 15-30 minutes depending on the cell line. Adding EDTA pH 8 to a final concentration of 5 mM stopped MNase digestion. The nuclei were then lysed by the addition of SDS to a final concentration of 0.5% and incubated with rotation for 1-2 hours at room temperature. This was followed by centrifugation at 2000xg for 5 minutes and the supernatant was diluted 5 fold with RIPA buffer supplemented with protease and phosphatase inhibitors.

After DNA fragmentation, the nuclear lysate was pre-cleared with the addition of 60 µL Protein A/G Plus agarose beads (Santa Cruz) per 1 mL of lysate and incubated for 1 hour at 4°C with rotation. The beads were pelleted by centrifugation at 1000xg for 3 minutes and the A_{260} of the lysate was measured. The lysate was aliquoted to several 1.5 mL microcentrifuge tubes containing equal amounts of A_{260} per tube. Additionally, 1-2 A_{260} of lysate was also saved as input. UCHL1 (mouse monoclonal antibody from R&D

Systems, MAB6007) or p53 (mouse monoclonal antibody from Abcam, ab28) antibody was added to the lysate at either 1:2 or 1:1 ratio (μg antibody: A_{260} of lysate), respectively. The antibody incubation was carried out overnight at 4°C with rotation. The following day, 7 μL of Dynabeads Protein G (Invitrogen) were added to each A_{260} of the lysate and incubated for 2-3 hours at 4°C with rotation. The beads were then washed twice with rotation at room temperature for 5-7 minutes with 1 mL of each of the following buffers: Low Salt wash buffer (0.1% SDS, 1% Triton-X-100, 2 mM EDTA, 20 mM Tris-pH 8.1 and 150 mM NaCl), High Salt wash buffer (0.1% SDS, 1% Triton-X-100, 2 mM EDTA, 20 mM Tris-pH 8.1 and 500 mM NaCl), LiCl wash buffer (250 mM LiCl, 1% NP-40, 1% deoxycholate, 1 mM EDTA and 10 mM Tris-HCl pH 8.1) and 1xTE buffer (10 mM Tris-HCl pH 7.5 and 1 mM EDTA). After washes, the antibody-chromatin complexes were eluted with the addition of 250 μL of elution buffer (1% SDS and 100 mM $NaHCO_3$) and incubated at room temperature for 30 minutes with rotation. The beads in elution buffer and the input sample were incubated overnight at 65°C to reverse the DNA-protein cross-links. The following day, the samples were treated with RNase A (0.02 μg/mL final concentration for 30 minutes at 37°C) and Proteinase K (0.5 μg/mL final concentration for 1 hour at 55°C). The ChIP and input DNA were purified by using the QIAquick PCR Purification Kit (Qiagen).

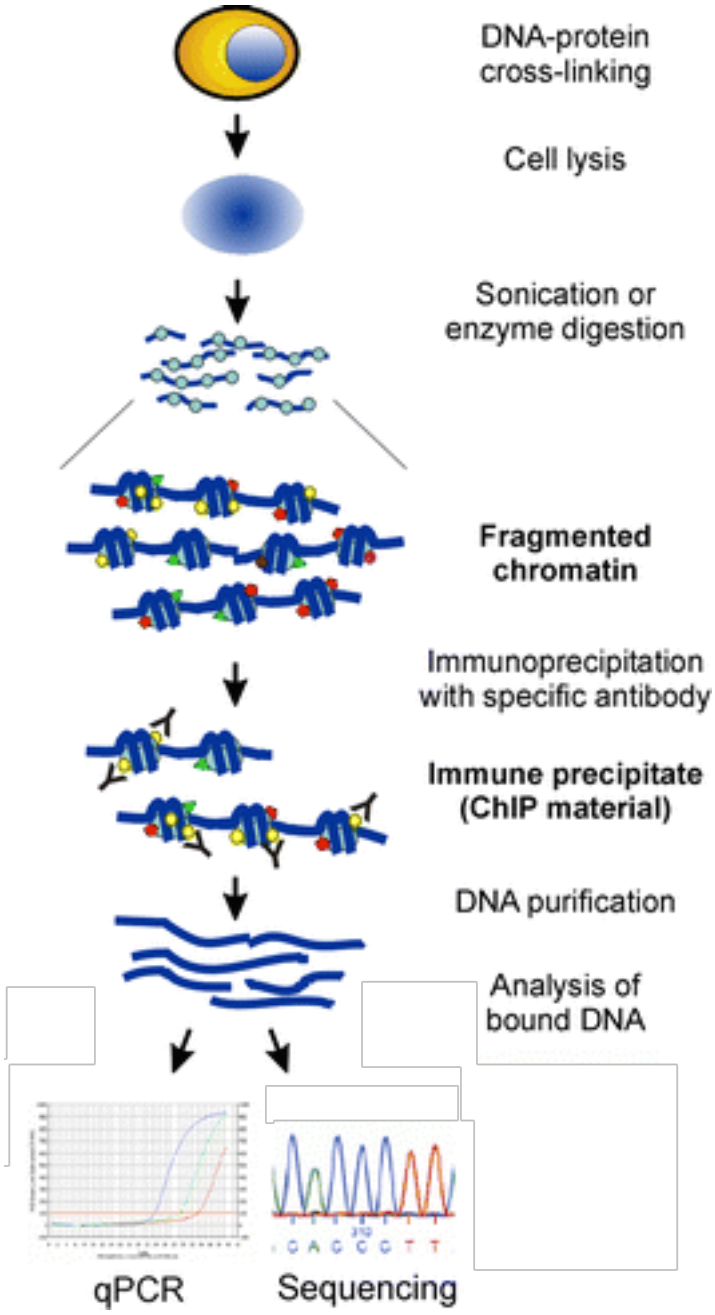

Figure 6. Schematic representation of the ChIP assay (Adapted from Collas, 2010).

3.5.2 ChIP-seq

3.5.2.1 DNA Preparation for SOLiD Sequencing

The ChIP and input DNA for ChIP-seq was purified by magnetic Agencourt AMPure XP beads (Beckman Coulter) as per manufacturer's instructions. The DNA was quantified by the Qubit 2.0 Fluorometer (Life Technologies). Carolina Gonzalez-Zuluaga performed the subsequent ChIP-seq library preparation steps according to the 5500 SOLiD fragment library protocol (Life technologies). The ChIP and input DNA size was first analyzed by the high sensitivity DNA kit and 2000 Bioanalyzer (Agilent Technologies). Approximately 20 ng of ChIP DNA was end-repaired and size selected (100-250 bp). This was followed by dA tailing and ligation of SOLiD barcodes. Finally, DNA libraries were prepared by ePCR and loaded onto the flowchip for sequencing by the SOLiD platform.

3.5.2.1 Bioinformatics Analyses

The following section was written by Dr Wayne Xu describing the methods used in analysis of the raw ChIP-seq data.

SOLiD sequence mapping

A total of 181,900,271 of 50-base SOLiD ChIP-seq sequence reads were generated from four DU145 cell samples, and 70,075,439 sequence reads from two HEK293T cell samples. We also analyzed three samples of 19,524,349 sequence reads of the SOLiD ChIP-seq data from NCBI GEo (GSE26005). All these sequences were ensured by quality check. The sequence reads were mapped on human reference genome

(hg19) using Lifescope v2.5.1 software (Life Technologies) with 2-mismatch settings. The color-based GSE26005 sequences were mapped using Bowtie version 2 instead (Langmead *et al.,* 2009).

Peak calling and annotation

The binding site candidates were identified by comparing ChIP sample to input sample using the model-based analysis of ChIP-Seq (MACS) peak caller with p-value 1e-5 and a mfold cutoff of high limit of 30 and low limit of 10 (Zhang *et al.,* 2008). We used the software CEAS to analyze the peak distribution among genome and their location regarding to genes (Shin *et al.,* 2009). We used Ensembl Human release 75 for gene annotations. We searched the binding site sequences against TRANSFAC data base (Biobase) by Match program with minimal false discovery rate of 0.1 cutoff. The common peaks among different samples were analyzed by custom script. We determined the two peaks were overlapped if one peak's center falls into another peak's range.

Data viewing

Browser views of gene tracks, ChIP-seq data and peaks are shown using Integrated Genomics Viewer (IGV) or using Partek Genomics Suite v6.6 (Partek Incorporated, St. Louis, Missouri, USA) (James *et al.,* 2011).

3.5.3 ChIP Optimization Steps

3.5.3.1 Cross-Linking of Cells

For a standard ChIP protocol, cells are usually cross-linked with 1% formaldehyde (Thermo Fisher Scientific) for 10 minutes at room temperature. Since it was unknown if UCHL1 is directly or indirectly associated with chromatin, cells were cross-linked by formaldehyde only as well as dual cross-linked by both 1 mM DSP (Thermo Fisher Scientific; 30 minutes at room temperature) and either 1% or 0.5% formaldehyde (10 minutes at room temperature).

3.5.3.2 DNA Fragment Size

3.5.3.2.1 Sonication

After cellular lysing and pelleting of the nuclei, nuclear pellets (usually 6 pellets containing approximately equal number of cells) were each resuspended in 1 mL of sonication buffer (10 mM Tris-HCl pH 7.5, 0.25 M sucrose and 75 mM NaCl) and SDS was added to a final concentration of 0.3%. With the addition of SDS, the nuclei were lysed at room temperature for 1-2 hours with rotation. All of the six 1.5 mL microcentrifuge were tubes cooled on ice. The 6 tubes were sonicated 5, 10, 15, 20, 25 and 30 times for 5 seconds each time at setting 3 with the sonicator (Fisher Scientific Model 100 Sonic Dismembrator). The tubes were kept on ice for approximately 30 seconds between each sonication cycle. After the appropriate number of sonication cycles, the tubes were centrifuged for 10 minutes at 17 000xg at 4°C. The supernatant was retained while the insoluble fraction was discarded. The supernatant was incubated at 65°C overnight to reverse the DNA to protein cross-links followed by RNase A (30

minutes at 37°C) and Proteinase K (1 hour at 55°C) treatments the following day. The DNA was purified using the PCR purification kit (Qiagen) and analyzed on an agarose gel or the bioanalyzer. This optimization protocol was repeated in case that DNA fragments were not the appropriate size, and more sonication cycles were performed until the desired size was obtained.

3.5.3.2.2 MNase Digestion

After cellular lysing and pelleting of the nuclei, a nuclear pellet was resuspended in the MNase digestion buffer and the A_{260} absorbance was measured. By quantifying the total A_{260}, it was possible to calculate the amount of MNase enzyme required at a concentration of 2.5 U/A_{260}. Once digestion has started, equal aliquots were taken from the reaction tube every 10 minutes (time points at 10, 20, 30, 40 and 50 minutes from the start of digestion). At each time point, the reaction was stopped with the addition of EDTA (5 mM final concentration) followed by the addition of SDS (0.5% final concentration). Nuclear lysis by SDS was performed at room temperature for 1-2 hours with rotation. This was followed by overnight 65°C incubation to reverse the DNA to protein cross-links followed by RNase A (30 minutes at 37°C) and Proteinase K (1 hour at 55°C) treatments the following day. The DNA for each time point was purified using the PCR purification kit (Qiagen) and analyzed on an agarose gel or the bioanalyzer. It is important to choose a specific MNase digestion time point that yields the highest amount of mononucleoseomes compared to polynucleosomes. Shorter time points are then chosen in the vicinity of the particular time point and the optimization process is repeated again to obtain a more specific time of MNase digestion. Alternatively, it is also possible

to choose the specific time point and then use a range of MNase concentrations but keep the time constant. In this case, concentrations in increments of 0.5 (1, 1.5, 2, 3, 3.5 and 4 etc.) were tested during the repeat of the MNase digestion optimization protocol.

3.5.3.3 Antibody Concentration

UCHL1 has not previously been described as a protein associated with DNA and hence there were no commercially available 'ChIP grade' antibodies available. Therefore, it was important the test numerous UCHL1 antibodies and determine if any are suitable for ChIP analyses. Firstly, antibodies suitable for immunoprecipitation and western blotting were obtained and given priority in the optimization tests. The first test was western blotting with the antibody to determine UCHL1 specificity in the desired cell line. Detecting only a single band at ~25 kDa shows that the antibody is specific to UCHL1 and can then be tested under ChIP conditions. After pre-clearing of the ChIP lysate and A_{260} quantification, 5 A_{260} of total ChIP lysate was aliquoted into each of three 1.5 mL microcentrifuge tubes (IP tubes). Also, 0.5 A_{260} (1/10 of IP) of ChIP lysate was kept as input. Different antibody amounts (µg antibody to A_{260} ratio) were then added to each of the three IP tubes at: 1:2 ratio (2.5 µg of antibody), 1:1 ratio (5 µg of antibody) and 2:1 ratio (10 µg of antibody). As described in Section 3.5.1, antibody incubation was performed overnight and magnetic beads were added the following day. After the 2-3 hour incubation with magnetic beads, an aliquot of each of the three immunodepleted (ID) fractions was kept (equal in volume to the input that was kept earlier in the protocol). After washes with Low Salt wash buffer, High Salt wash buffer, LiCl wash buffer and 1xTE buffer, SDS-PAGE loading buffer was added to the washed magnetic

beads-antibody-UCHL1 complex. The SDS-PAGE loading buffer was also added to the input and three ID fractions. All were boiled for 5 minutes and loaded onto a polyacrylamide gel. After western blotting, the intensity of the IP and ID bands was compared to the input band. The IP band representing a specific 'μg antibody to A_{260} ratio' that shows the most enrichment compared to input as well as the least protein in the corresponding ID lane was picked for subsequent ChIP analyses. In case there was no enrichment of UCHL1 detected compared to the input lane or the IP lanes were clear, this was an indication that the antibody was not suitable for ChIP. This could be due to the high stringency of the RIPA buffer used for ChIP or the subsequent stringent washing steps. If this was the case, other UCHL1 antibodies were tested until finding an antibody suitable for ChIP.

3.5.3.4 Duration of Reverse Cross-Linking

Previous preliminary data has suggested that the duration of reversal of DNA to protein cross-links plays a role in the yield of ChIP DNA obtained as well as potential DNA aggregation due to extended reversal time. Once the ChIP lysate (Input) was prepared, it was divided into equal aliquots each representing a specific time point. The DNA to protein cross-links were reversed at 65°C in a water bath. After each time point, the corresponding aliquot was treated with RNase A (30 minutes at 37°C) followed by Proteinase K (1 hour at 55°C). The DNA was purified using the PCR purification kit (Qiagen) and analyzed on an agarose gel or the bioanalyzer.

3.6 5-Aza-2'-Deoxycytidine Treatments

The human prostate cancer cell lines DU145, PC3, LNCaP and C4-2 were split to a low density and left to attach overnight. The 5-aza-2'-deoxycytidine (Sigma) was dissolved in DMSO and 100 mM stock was prepared. The cell culture media was aspirated the following day and replaced with media supplemented with 5-aza-2'-deoxycytidine. Four different treatments were performed including: the Mitsui *et al.,* 2012 method where cells are treated once with 5 μM 5-aza-2'-deoxycytidine for 4 days; the Chiam *et al.,* 2011 method where new media containing 0.5 μM 5-aza-2'-deoxycytidine was changed every day for 6 days; a method where the cells were grown for 3 passages (6 days) in media containing 10 μM 5-aza-2'-deoxycytidine; and a co-treatment described by Walton *et al.,* 2008 where the cells were treated once with 8.8 μM 5-aza-2'-deoxycytidine for 72 hours followed by the addition of 300 nM TSA for an additional 24 hours. After treatment, the cells were washed twice with 1xPBS and harvested. From cell pellets, total cellular lysates and total RNA were extracted, which were used for western blot and RT-PCR analyses, respectively.

3.7 Polymerase Chain Reaction (PCR)

3.7.1 Reverse Transcription Polymerase Chain Reaction (RT-PCR)

Total RNA was extracted from both untreated and epigenetic drug treated DU145, PC3, LNCaP and C4-2 cells using the RNeasy Plus Mini Kit (Qiagen) as per the manufacturer's instructions. The RNA concentration and purity based on the A_{260}/A_{280} ratio was measured by Nanodrop 2000 (Thermo Fisher Scientific). The cDNA synthesis was performed with M-MLV reverse transcriptase kit and oligo $(dT)_{12-18}$ in accordance

with the manufacturer's instructions (Invitrogen). Multiplex RT-PCR was performed with either *UCHL1* and *GAPDH* or *GSTP1* and *GAPDH*. The primers used for RT-PCR analyses are shown in Table 1. The RT-PCR products were run on a 1% agarose gel.

Table 1. List of Primers Used in RT-PCR Analyses

Name	Sequence
UCHL1 (Forward)	5'-CAGAGAAAATGTCCCCTGAAGACAG-3'
UCHL1 (Reverse)	5'-CAGAGAGCCACGGCAGAGAAG-3'
GAPDH (Forward)	5'-TTCGTCATGGGTGTGAACCATGAG-3'
GAPDH (Reverse)	5'-CTGCTTCACCACCTTCTTGATGTC-3'
GSTP1 (Forward)	5'-GACCTTCATTGTGGGAGACCAGATC-3'
GSTP1 (Reverse)	5'-TTGCCATTGATGGGGAGGTTCAC-3'

3.7.2 Real-Time Polymerase Chain Reaction (qPCR)

The qPCR analyses were performed using the Bio-rad CFX96 Real-Time PCR Detection System. The qPCR reactions were prepared in 96-well plates on ice. The reactions were prepared to a total volume of 50 µL using equal masses of 0.5-1.0 ng for ChIP and input DNA whereas the IgG control DNA was added in equal volume to ChIP and input DNA (10 µL). The primers used for qPCR analyses are shown in Table 2.

Table 2. List of Primers Used in qPCR Analyses

Name	Sequence
CDKN1A p53 binding site 2 (Forward)	5'-AAACAGGCAGCCCAAGGACA-3'
CDKN1A p53 binding site 2 (Reverse)	5'-TGGCTCTGATTGGCTTTCTG-3'
CDKN1A p53 binding site 3 (Forward)	5'-CGTTAGAGGAAGAAGACTG-3'
CDKN1A p53 binding site 3 (Reverse)	5'-AGCAGCTACAATTACTGACA-3'
BAX p53 binding site (Forward)	5'-GGCTCACAAGTTAGAGACAAGC-3'
BAX p53 binding site (Reverse)	5'-CCAGGCAGGACGTTATAGATGA-3'

Chapter 4: Results

4.1 UCHL1 is Associated with Genomic DNA

In order to identify proteins differentially cross-linked to genomic DNA by cisplatin in BPH1, LNCaP, DU145 and PC3 cell lines, Sumin Lu from the Davie lab compared 2D gel patterns of cisplatin cross-linked proteins. The proteins cross-linked to DNA by cisplatin were captured on hydroxyapatite, and the protein-DNA cross-linking was reversed with thiourea. The isolated proteins were then resolved using 2D PAGE. One of the proteins (Spot 16) bound to nuclear DNA was present in DU145 but absent from BPH1, LNCaP and PC3 cell lines. Mass spectrometry analyses (in-gel digestion, nano-liquid chromatography and tandem mass spectrometry) identified 'Spot 16' as a protein with a molecular mass of 24.8 kDa and a pI of 5.33 (Figure 7). This protein was identified as UCHL1.

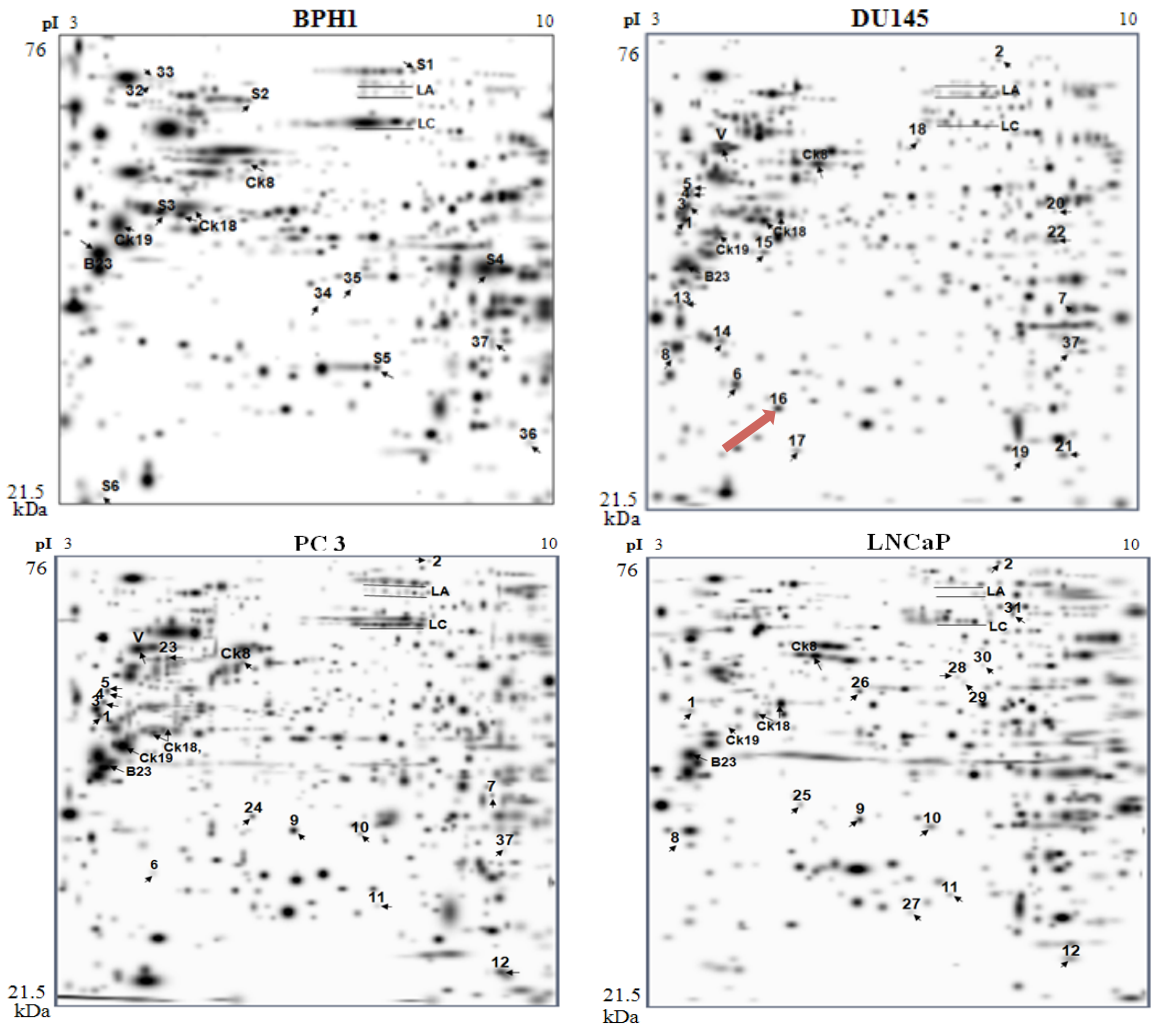

Figure 7. 2D gel patterns of proteins cross-linked to DNA by cisplatin *in situ* in BPH1 and DU145, PC3 and LNCaP prostate cancer cell lines. UCHL1 is cross-linked to DNA only in DU145 (Shown as 'Spot 16') (Sumin Lu).

Western blot analyses with an anti-UCHL1 antibody were performed to verify the mass spectrometry findings. Isolated proteins from cisplatin cross-linked cells were resolved by SDS-PAGE and immunoblotted. The results were consistent with the mass spectrometry findings where UCHL1 is only cross-linked to DNA in DU145 prostate cancer cells (Figure 8A). Histone deacetylase 1 (HDAC1) was used as a reference since it was previously shown to be readily cross-linked to DNA by either cisplatin or

formaldehyde. Formaldehyde cross-linking, as in the ChIP assay, was also performed with DU145, BPH1, LNCaP and PC3 cells where once again it was confirmed that UCHL1 was only bound to nuclear DNA in the brain metastasis DU145 prostate cancer cell line (Figure 8B). Sumin Lu performed all the analyses described above.

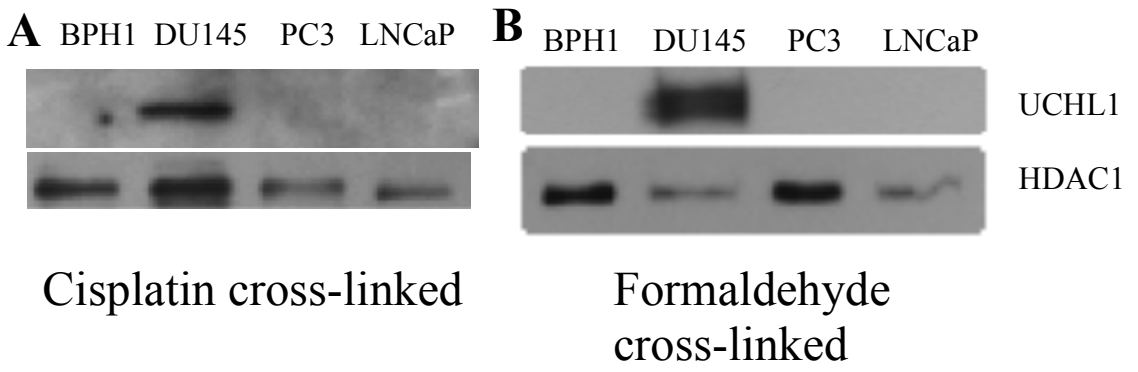

Figure 8. UCHL1 is cross-linked to DNA by cisplatin (A) and formaldehyde (B) *in situ* in DU145 prostate cancer cell line only (Sumin Lu).

To determine the UCHL1 protein expression, total cell lysates from BPH1, DU145, LNCaP, PC3 and C4-2 cell lines were prepared. The lysates were resolved by SDS-PAGE followed by western blot analysis with an anti-UCHL1 antibody. Interestingly, UCHL1 is only expressed in the DU145 prostate cancer cell line and not expressed in BPH1 or LNCaP, PC3 and C4-2 prostate cancer cell lines (Figure 9).

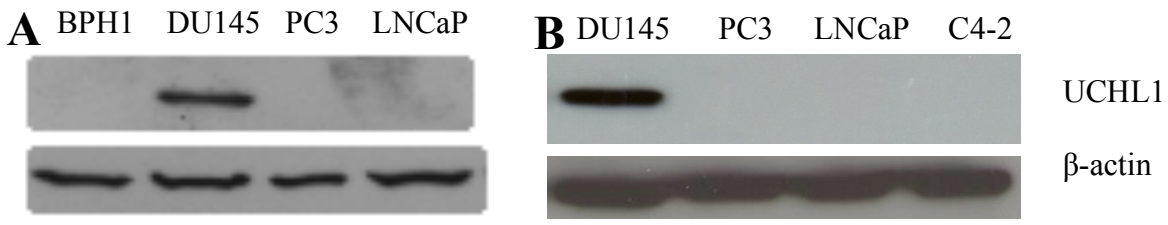

Figure 9. UCHL1 protein is expressed in DU145 prostate cancer cell line only. Total cell lysates of BPH1, DU145, PC3 and LNCaP (A; Sumin Lu) and DU145, PC3, LNCaP and C4-2 (B) were resolved by SDS-PAGE followed by western blot analyses. This experiment was reproducible and consisted of three biological replicates.

4.2 UCHL1 Expression Is Not Induced in PC3, LNCaP and C4-2 Prostate Cancer Cell Lines After 5-Aza-2'-Deoxycytidine Treatment

It has previously been reported that the UCHL1 gene in prostate and other cancers is supressed by upstream promoter methylation (Mitsui *et al.,* 2012; Tokumaru *et al.,* 2008). Since this was the case, prostate cancer cells that did not express UCHL1 (PC3, LNCaP and C4-2) were treated with epigenetic drugs to induce UCHL1 expression. The aim of this experiment was to induce the expression of UCHL1 and subsequently determine if the induced UCHL1 protein would be associated with genomic DNA, as is the case with DU145 cells.

As previously described in Section 3.5, four different treatments were performed. These include: the Mitsui *et al.,* 2012 method where cells are treated once with 5 μM 5-aza-2'-deoxycytidine for 4 days; the Chiam *et al.,* 2011 method where new media containing 0.5 μM 5-aza-2'-deoxycytidine was changed every day for 6 days; a method where the cells were grown for 3 passages (6 days) in media containing 10 μM 5-aza-2'-deoxycytidine; and a co-treatment described by Walton *et al.,* 2008 where the cells were treated once with 8.8 μM 5-aza-2'-deoxycytidine for 72 hours followed by the addition of 300 nM TSA for an additional 24 hours. TSA is an HDAC inhibitor and was used in

combination with 5-aza-2'-deoxycytidine due to the fact that a repressive complex may silence certain tumour suppressor genes. The complex is comprised of DNA methyltransferase 1, histone deacetylases (HDACs) and polycomb (PcG) proteins. After treatment, the total cell lysates and total RNA were isolated for SDS-PAGE and western blot analyses or RT-PCR analyses. It is important to note that all treatments produced identical results and showed that neither the UCHL1 protein (Figure 10A) nor mRNA (Figure 10B) expression was induced after treatment. An anti-GSTP1 antibody and *GSTP1* primers were used in order to determine whether GSTP1 (glutathione S-transferase pi 1) was induced after 5-aza-2'-deoxycytidine treatment (Figure 4). GSTP1 was previously used as a marker for 5-aza-2'-deoxycytidine treatment efficacy in LNCaP prostate cancer cells (Chiam *et al.,* 2011). GSTP1 was expressed in DU145 and PC3 prostate cancer cells but not in LNCaP and C4-2 prostate cancer cells due to promoter hypermethylation. After 5-aza-2'-deoxycytidine treatment, GSTP1 expression was induced in LNCaP and C4-2 cells confirming that the 5-aza-2'-deoxycytidine treatment was effective but unable to induce UCHL1 expression in LNCaP, PC3 or C4-2 prostate cancer cells.

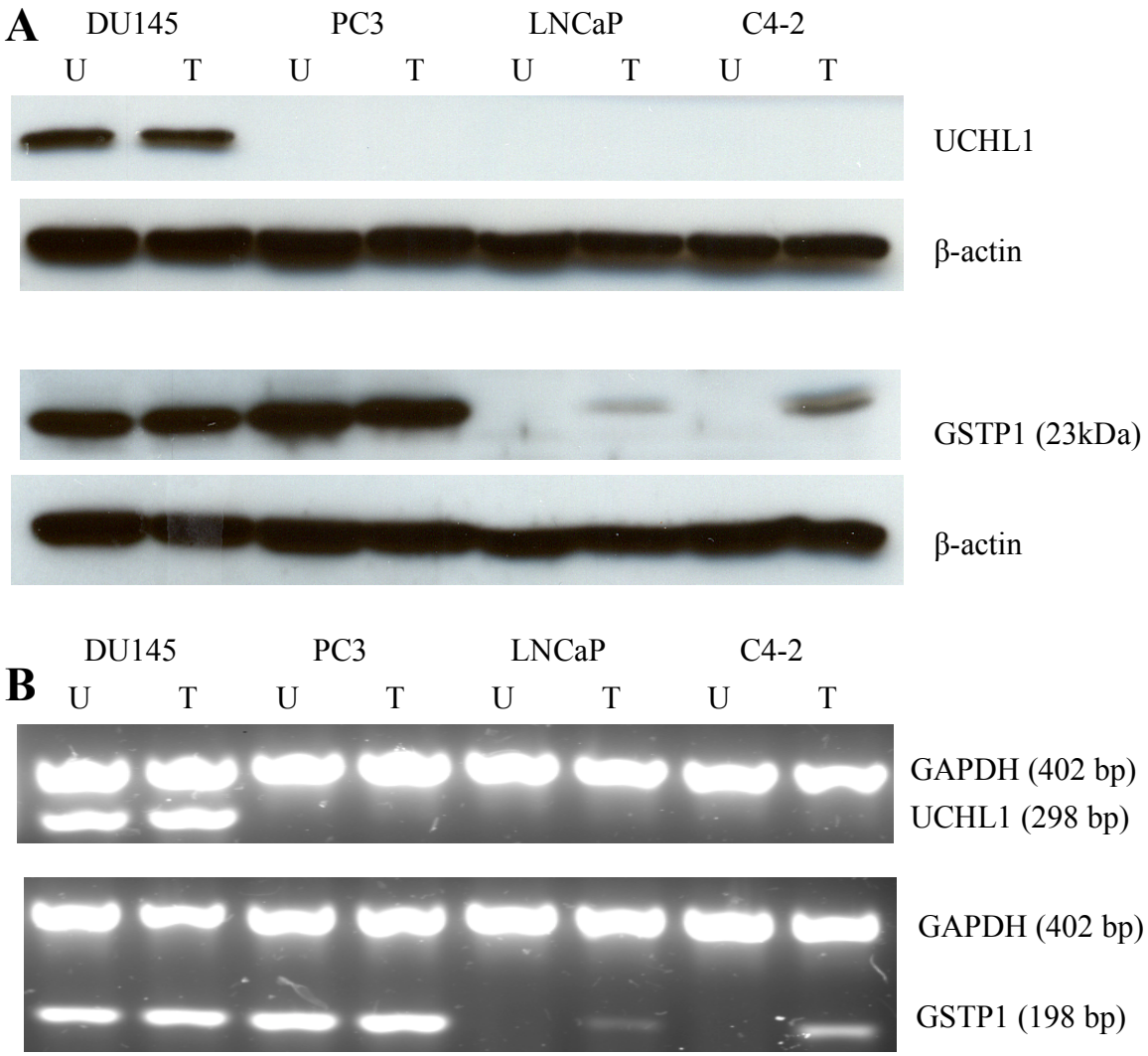

Figure 10. UCHL1 protein (A) and mRNA (B) expression before (U: untreated) and after 5-aza-2'-deoxycytidine (and TSA) treatments (T: treated) in DU145, PC3, LNCaP and C4-2 cells. GSTP1 was used as a marker for 5-aza-2'-deoxycytidine treatment efficacy in LNCaP and C4-2 prostate cancer cells where it is not expressed. β-actin was used as a loading control for western blot and GAPDH was used as a control for RT-PCR. This experiment was reproducible and consisted of three biological replicates.

4.3 UCHL1 Is Associated with p53 but UCHL1 and p53 Do Not Bind to Genomic DNA of Upstream Promoter Regions of *CDKN1A* and *BAX* genes

Previous immunoprecipitation studies have demonstrated that UCHL1 interacts with p53 (Li *et al.,* 2010; Yu *et al.,* 2008). Co-IP and immunoblot analyses have demonstrated that UCHL1 interacts with p53 in DU145 prostate cancer cells. This result

was obtained by immunoprecipitating p53 from DU145 total cell lysate and performing immunoblot analyses with antibodies raised against UCHL1 and p53 (Figure 11A). The reciprocal immunoprecipitation experiment was also performed (Figure 11B). Comprehensive optimization analyses were performed to obtain an antibody appropriate for UCHL1 IP experiments. Numerous antibodies raised against UCHL1 were tested under low stringency IP conditions but immunoprecipitation of UCHL1 was unsuccessful. Upon learning the unique protein structure of UCHL1, it was hypothesized that UCHL1 was not able to be immunoprecipitated under low stringency conditions due to the antibody epitope being masked as a result of the UCHL1 complex knotted structure or perhaps due to an interaction with another protein. DSP cross-linker was used to covalently cross-link interacting proteins followed by high stringency IP. The DSP cross-linking was a necessary step allowing for immunoprecipitation of UCHL1 under high stringency conditions while retaining protein-protein interactions. This approach confirmed once again that there was an interaction between UCHL1 and p53 allowing for further ChIP analyses.

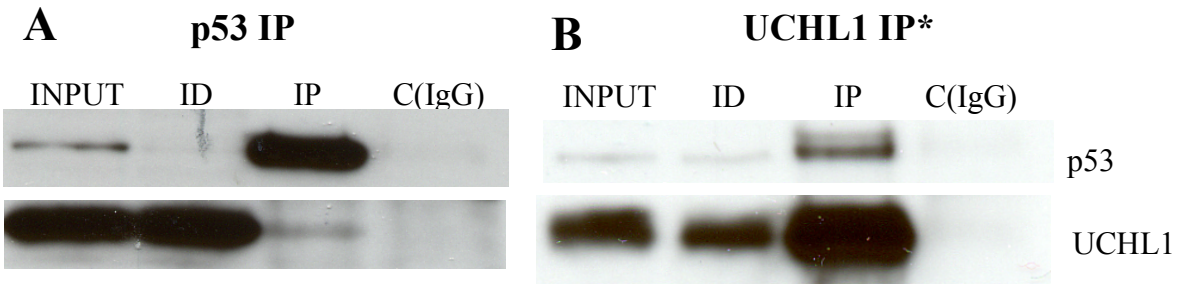

Figure 11. UCHL1 interacts with p53 in DU145 prostate cancer cells. p53 IP performed with normal DU145 cells (total cell lysates) and WB with p53 and UCHL1 antibodies (A). UCHL1 IP (*high stringency IP) performed with DU145 cells cross-linked with DSP (total cell lysates in RIPA buffer) and WB with UCHL1 and p53 antibodies (B). Equal volumes of input total cell lysate, ID (immunodepleted fraction), IP and C (control IgG from the same species as IP antibody) were loaded to each lane. This experiment was reproducible and consisted of three biological replicates.

Since UCHL1 was shown to interact with p53, subsequent ChIP assays were performed to determine whether these proteins co-localize on genomic DNA. Two genes regulated by p53 have been chosen for this study, *CDKN1A* and *BAX*. *CDKN1A* codes for the cell cycle regulator $p21^{Waf1}$ and has three known p53 binding sites, while *BAX* codes for a pro-apoptotic BCL2 family member and has two overlapping p53 binding sites (Beckerman and Prives, 2010). Also, in case UCHL1 was recruited to DNA by a transcription factor (i.e. p53), dual cross-linking was also performed with both DSP and formaldehyde to cross-link UCHL1 to the transcription factor and then cross-link the complex to DNA. The ChIP DNA was isolated and interrogated with primers placed on either side of known p53 DNA binding sites in the upstream promoter regions of *CDKN1A* and *BAX* genes in DU145 prostate cancer cells. Initially, p53 ChIP was performed to determine whether p53 binds to these regions. Only two of the p53 *CDKN1A* binding sites were tested as the third site is located in GC-rich regions and qPCR was unsuccessful requiring a unique qPCR protocol specialized for these regions. Due to the complex nature of this protocol, the study was focused on only two of the p53 binding sites on the *CDKN1A* upstream promoter. However, qPCR analyses with p53 ChIP DNA did not show enrichment at p53 binding sites on the *CDKN1A* and *BAX* upstream promoter regions in the cycling DU145 cells (Figure 12). UCHL1 ChIP was also attempted followed by qPCR analysis with primers for the *BAX* upstream promoter regions. Similarly, qPCR with UCHL1 ChIP DNA did not show enrichment at these p53 binding sites (Figure 13). ChIP with dual cross-linked DU145 cells was also performed and also yielded almost identical results.

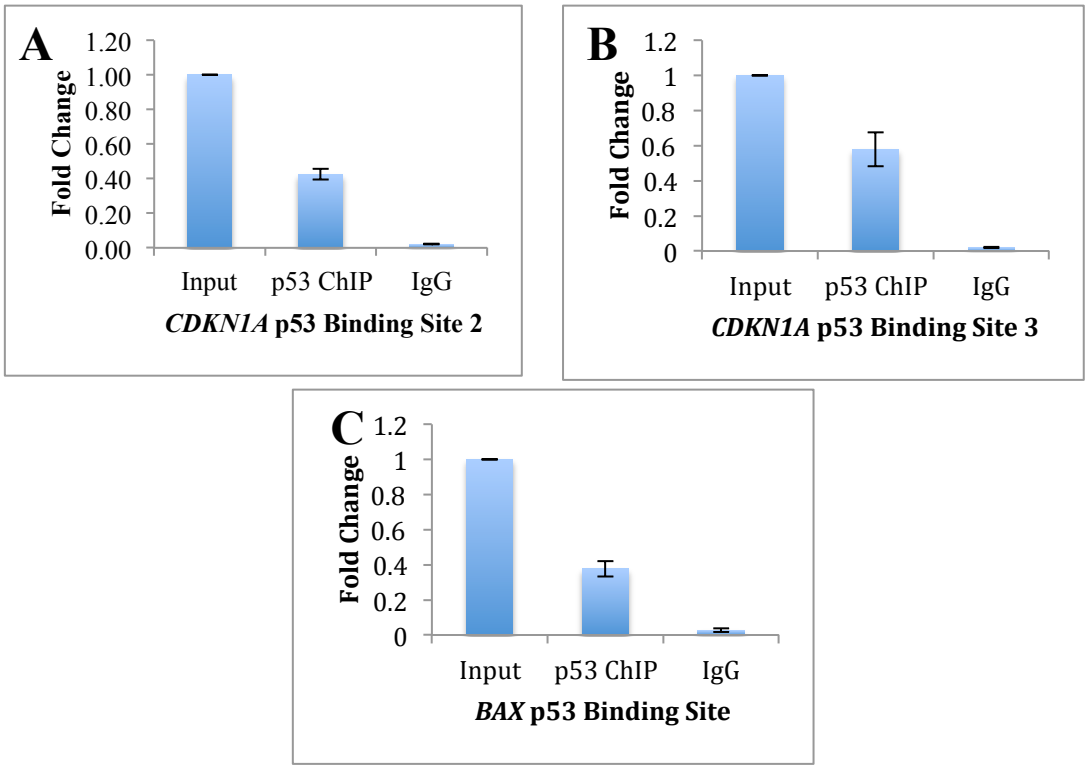

Figure 12. qPCR fold enrichment relative to input DNA of p53 ChIP DNA at p53 binding sites on the *CDKN1A* (A and B) and *BAX* (C) upstream promoter regions ± standard deviation (n=3).

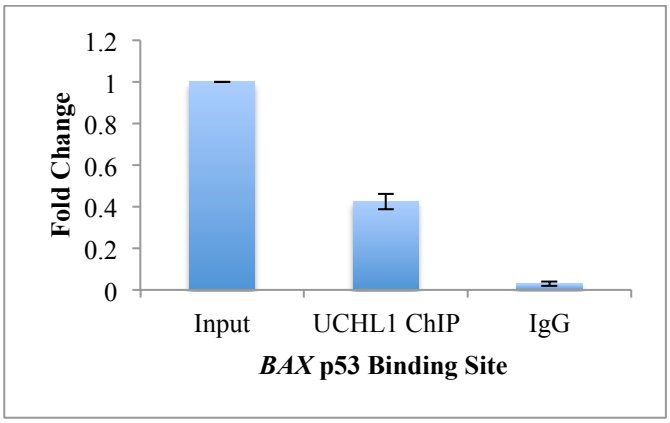

Figure 13. qPCR fold enrichment relative to input DNA of UCHL1 ChIP DNA at p53 binding sites on the *BAX* upstream promoter regions ± standard deviation (n=3).

The HEK293T cell line was also used since Bheda *et al.,* 2009b had shown that UCHL1 knockdown in these cells controls the expression of genes like *CDKN1A* and *BAX*. It was important to determine whether the interaction of UCHL1 and p53 is the mechanism behind the expression of these genes. The same analyses with HEK293T cells under formaldehyde only and dual cross-linking conditions with DSP and formaldehyde were performed. Once again, the results were almost identical qPCR analyses with p53 ChIP DNA did not show enrichment at p53 binding sites on the *CDKN1A* and *BAX* upstream promoter regions suggesting p53 does not bind to these regions or binding levels are very low.

The fact that p53 is mutated in DU145 leads to the assumption that its DNA binding may be affected and considerably reduced. Also, studies involving p53 DNA binding were performed under stress conditions by stimulating the cells with stress agents. Since UCHL1 was shown to be cross-linked to DNA under normal unstimulated physiological conditions, it was decided to not pursue p53 targets further but rather focus on the unbiased screening approach, ChIP-seq.

4.4 UCHL1 ChIP-seq

4.4.1 UCHL1 ChIP-seq in 1% Formaldehyde Cross-Linked DU145 Cells

As mentioned in Section 3.4 thorough optimization steps, including cell cross-linking, DNA fragmentation, antibody optimization and the duration of reverse cross-linking, were taken to successfully complete ChIP-seq. The DNA from cross-linked DU145 cells was fragmented by shearing (sonication) and multiple sonication times were tested to obtain suitable DNA fragments of 250-300 bp in length. The length of DNA was

determined by agarose gel electrophoresis or bioanalyzer analyses. Also, numerous commercially available UCHL1 antibodies were tested under ChIP conditions to obtain a suitable 'ChIP-grade' UCHL1 antibody. Other factors that were also taken into consideration and optimized were the amount of starting material per assay (number of cells), cross-linking time and time of reverse cross-linking. It was vital to successfully complete these ChIP optimization steps to allow for successful immunoprecipitation, purification and sequencing of the ChIP DNA.

After ChIP-seq and bioinformatic data analysis, the UCHL1 ChIP-seq of formaldehyde cross-linked DU145 prostate cancer cells identified approximately 1000 peaks. The regions where UCHL1 was potentially binding on the genomic DNA were highly repetitive and not located in the gene regulatory regions but rather intergenic. These sequences contained a CCC (GGG) repeat every three bases. With the help of bioinformatician Dr Wayne Xu, three potential UCHL1 binding sites were selected for further validation. All of these peaks were located in the intronic regions of three different genes: DDX11L2, FAM157A and RASGRF1. Due to the highly repetitive nature of the UCHL1 ChIP-seq peaks, primer design was difficult and validation of these peaks by qPCR was unsuccessful. The repetitive nature of the sequences and qPCR validation failure cast doubt over the validity of the ChIP-seq data. It was then decided to repeat ChIP-seq using dual cross-linking as UCHL1 likely interacts with DNA indirectly.

4.4.2 UCHL1 Shows Higher Association with DNA in Dual Cross-Linked Cells

Following the initial ChIP-seq with 1% formaldehyde cross-linked DU145 cells, it was decided to do ChIP-seq under dual cross-linked conditions. The protocol using

hydroxyapatite isolation of DNA cross-linked proteins was initially performed with dual cross-linked DU145 and HEK293T cells. This proved to be a superior cross-linking method since it was demonstrated that more UCHL1 protein was associated with DNA under dual cross-linking conditions (Figure 14). This suggests that UCHL1 is also indirectly bound to DNA through another DNA binding protein or a protein complex and allowed for further UCHL1 ChIP-seq analyses with dual cross-linked DU145 and HEK293T cells.

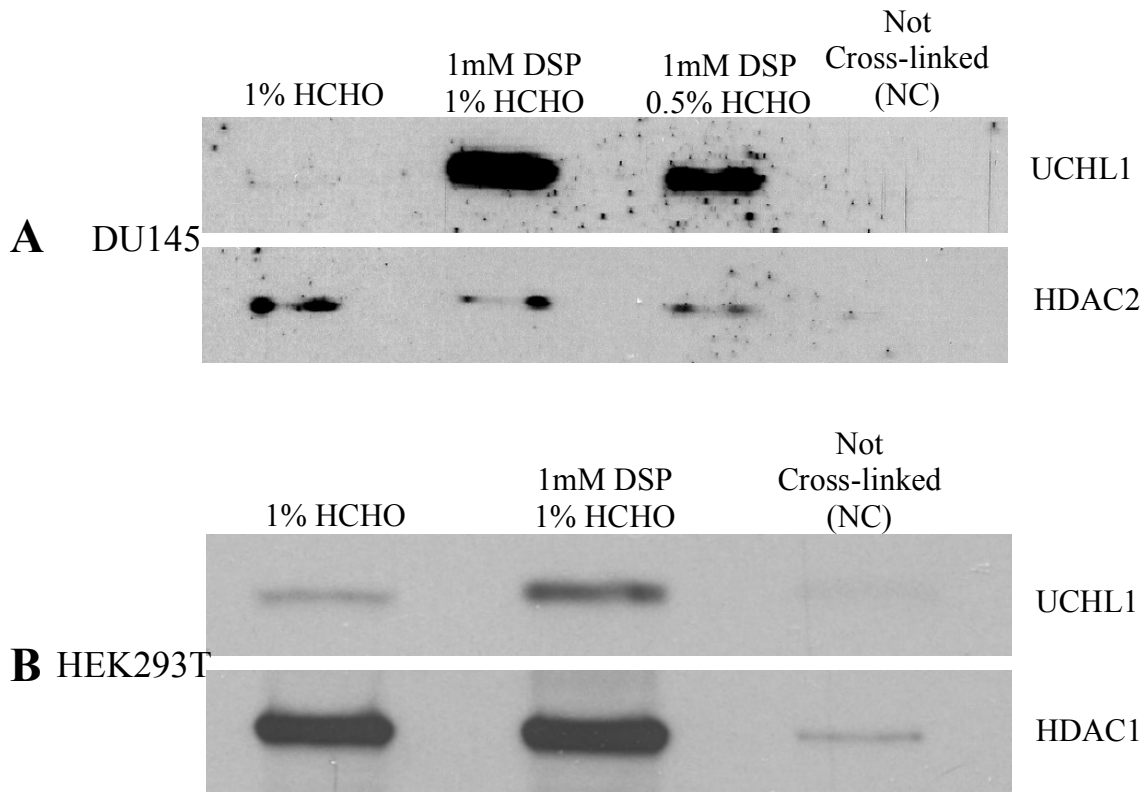

Figure 14. Isolation of DNA bound UCHL1 protein by hydroxyapatite from formaldehyde only (1% HCHO), dual cross-linked (DSP and HCHO) and not cross-linked (NC) DU145 (A) and HEK293T (B) cells. This experiment was reproducible and consisted of three biological replicates.

4.4.3 UCHL1 ChIP-seq in Dual Cross-Linked DU145 and HEK293T Cells

UCHL1 ChIP DNA was isolated from dual cross-linked DU145 and HEK293T cells and sequenced by next generation DNA sequencing using a SOLiD sequencer. The sequences were mapped against the human genome hg19 assembly. This time the HEK293T cell line was also used since Bheda *et al.,* 2009b have reported that UCHL1 knockdown in HEK293T cells influences the expression of pro- and anti-apoptotic genes. ChIP-seq analyses will be able to determine whether UCHL1 is associated with the regulatory regions of these genes and thus potentially have a role in their expression. Similarly to the first ChIP-seq run (Section 4.4.1), the UCHL1 bound peak sequences from dual cross-linked DU145 and HEK293T cells were highly repetitive. By using the default cutoff p-value of 1e-05, there were 2196 UCHL1 ChIP-seq peaks in HEK293T cells and 1532 UCHL1 ChIP-seq peaks in DU145 cells. Also, the UCHL1 bound peaks of target regions from dual cross-linked DU145 and HEK293T cells matched multiple peaks from the formaldehyde only cross-linked DU145 cells. To determine the number of overlapping UCHL1 ChIP-seq peaks between the cell lines and cross-linking conditions, the sequencing data was filtered (peak size ≥75 bp and reads coverage ≥10). This resulted in 1372 UCHL1 ChIP-seq peaks in HEK293T cells, 467 UCHL1 ChIP-seq peaks in DU145 cells and 293 peaks in formaldehyde only cross-linked DU145 cells. As shown in Figure 15, there were 60 common UCHL1 binding sites (peaks) between dual cross-linked DU145 and HEK293T cells. Additionally, there were 27 common UCHL1 binding sites between dual cross-linked DU145 and HEK293T cells and the formaldehyde only cross-linked DU145 cells (Figure 15).

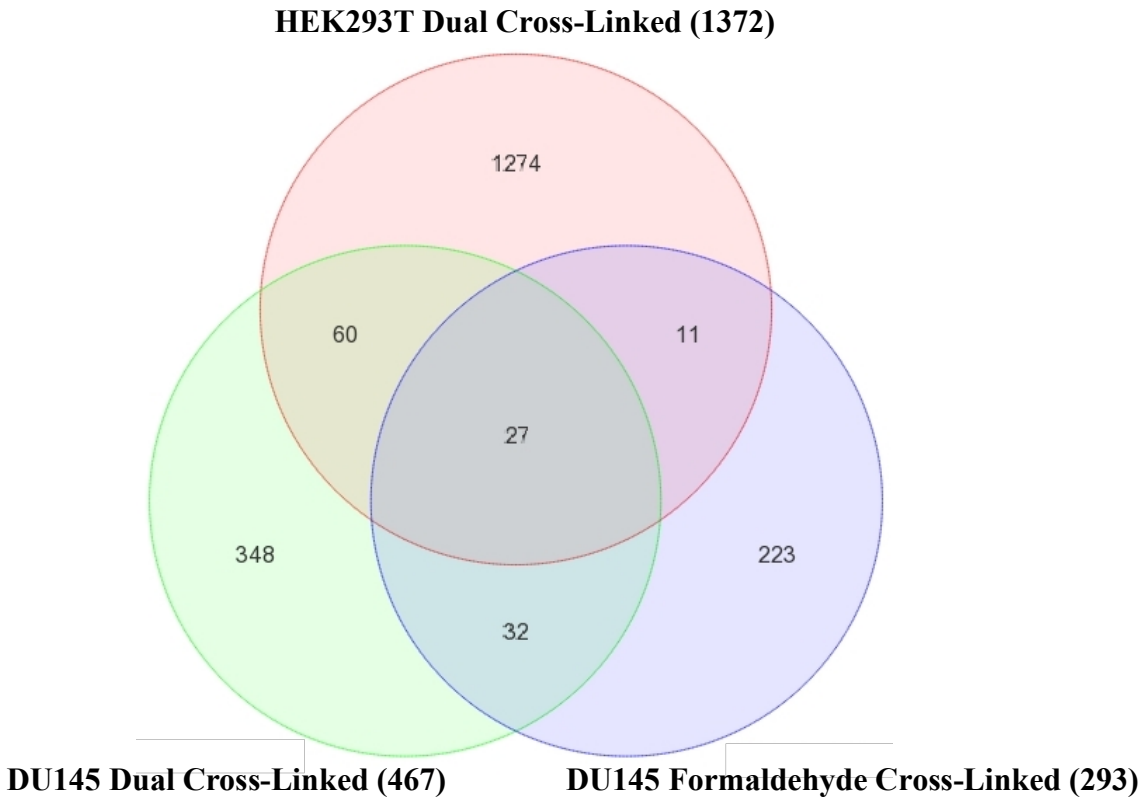

Figure 15. Venn diagram of overlapping UCHL1 ChIP-seq peaks between dual cross-linked DU145 (467 peaks) and HEK293T (1372) cells and the formaldehyde only cross-linked DU145 (293) cells (data has been filtered where peak size is ≥75 bp and reads coverage is ≥10).

There were 461 peaks from the dual cross-linked DU145 cells that were annotated to genes, meaning they were within the gene body or within 3,000 bp of a gene. The majority of the ChIP-seq peaks were in two categories where 33.4% were within intronic regions and 58.4% were in distal intergenic regions (>3,000 bp from a gene). The ChIP-seq of dual cross-linked HEK293T cells showed that 1394 peaks were annotated to genes. Similarly to DU145 cells, 24.1% were in intronic regions and 56.5% were in distal intergenic regions (Figure 16).

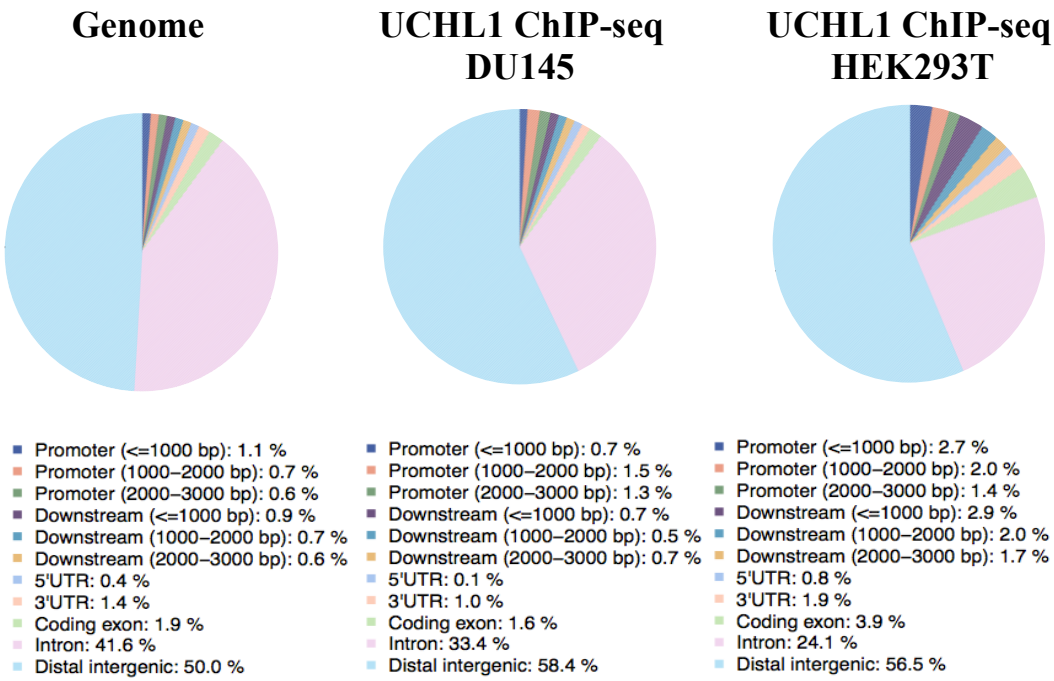

Figure 16. Genomic distribution of UCHL1 ChIP-seq peaks from dual cross-linked DU145 and HEK293T cells relative to the genome. The UCHL1 ChIP-seq peaks were located within a promoter (up to 3000 bp from a gene); up to 3000 bp downstream of a gene; the 5' untranslated region (UTR) or 3' UTR; within exons or introns; and distal intergenic regions where the peak is located more than 3000 bp from a gene.

The DNA associated with UCHL1 binding sites from dual cross-linked DU145 and HEK293T cells contained the CCCTAA (TTAGGG) repeat. Since this was the case, the underlying sequence of the peak of one of the target genes, DDX11L2, was inputted into the TRANSFAC database. This approach identified if other proteins such as transcription factors bind to these repetitive sequences and if potentially UCHL1 is indirectly associated with DNA through these proteins. The *in silico* search of transcription factors potentially binding to the UCHL1 binding sites identified TRF1 (telomeric repeat binding factor 1). TRF1 is part of the shelterin complex along with TRF2, TIN2, TPP1, POT1 and RAP1. *In silico* searches led to a published study by Lee *et al.,* 2011, which identified over 300 proteins that were associated with the shelterin

complex. According to the study, UCHL1 was associated with RAP1 and TIN2 proteins, which is the first time this interaction was documented.

Further literature searches identified two publications in which ChIP-seq of the shelterin complex proteins was performed. Yang *et al.,* 2011 reported on RAP1 and TRF2 ChIP-seq target sites in HTC75 cells while Simonet *et al.,* 2011 performed TRF1 and TRF2 ChIP-seq in transformed BJ fibroblast cells. One of the RAP1 binding sites from the Yang *et al.,* 2011 ChIP-seq data was shown to bind to an intron of the *CLIC6* gene. By looking up the exact genomic location of this peak compared to the UCHL1 ChIP-seq data, I discovered that the RAP1 and UCHL1 bind to the identical genomic region. The same was also seen in regards to the *FAM157A* gene. This suggests that UCHL1 and RAP1 co-localize to the same genomic regions.

The Simonet *et al.,* 2011 study did not specify the exact locations of ChIP-seq peaks but rather had uploaded the raw sequencing data to the GEO (Gene Expression Omnibus) database. This allowed Dr Wayne Xu to map the TRF1 and TRF2 ChIP-seq sequence reads to the hg19 human reference genome. Likewise, the UCHL1 ChIP-seq sequence reads from formaldehyde cross-linked DU145 cells and dual cross-linked DU145 and HEK293T cells were also mapped. It was evident that DNA associated with the UCHL1 binding sites aligned to the same genomic locations of TRF1 and TRF2 peaks, once again suggesting that UCHL1 co-localizes to the same genomic locations as the shelterin complex. The underlying sequences of these peaks also contained telomeric repeat sequences, CCCTAA (TTAGGG). The peaks were located in close proximity to telomeres and also contained interstitial telomeric sequences (ITSs). Some examples include the intronic region of the *CLIC6* (Figure 16A) and *FAM157A* (Figure 16B) genes

but also in distal intergenic regions of chromosomes 10 (Figure 16C) and 12 (Figure 16D). The UCHL1, TRF1 and TRF2 peak from chromosome 10 is an ITS while the UCHL1, TRF1 and TRF2 peak from chromosome 12 is located in close proximity to the telomere.

A

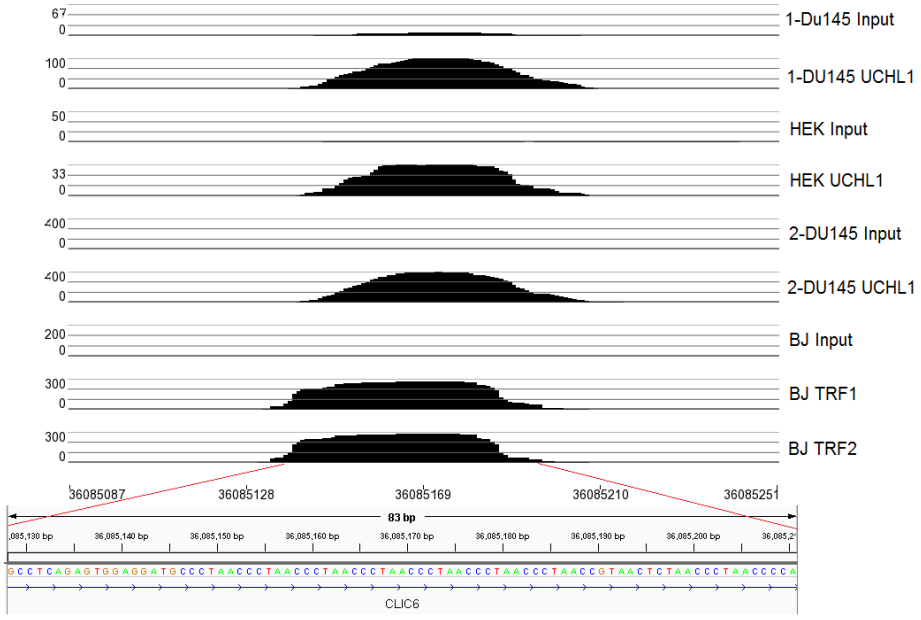

B

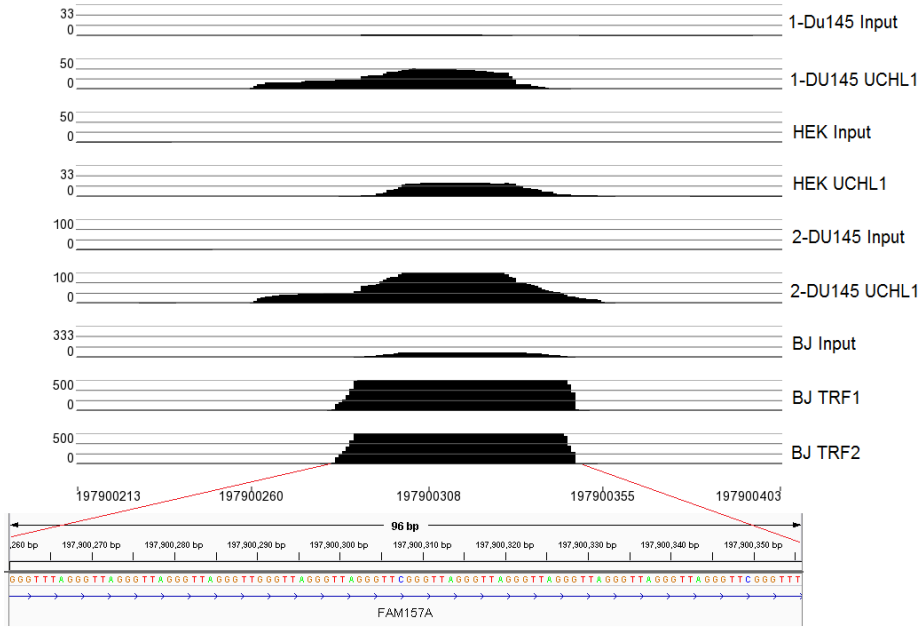

C

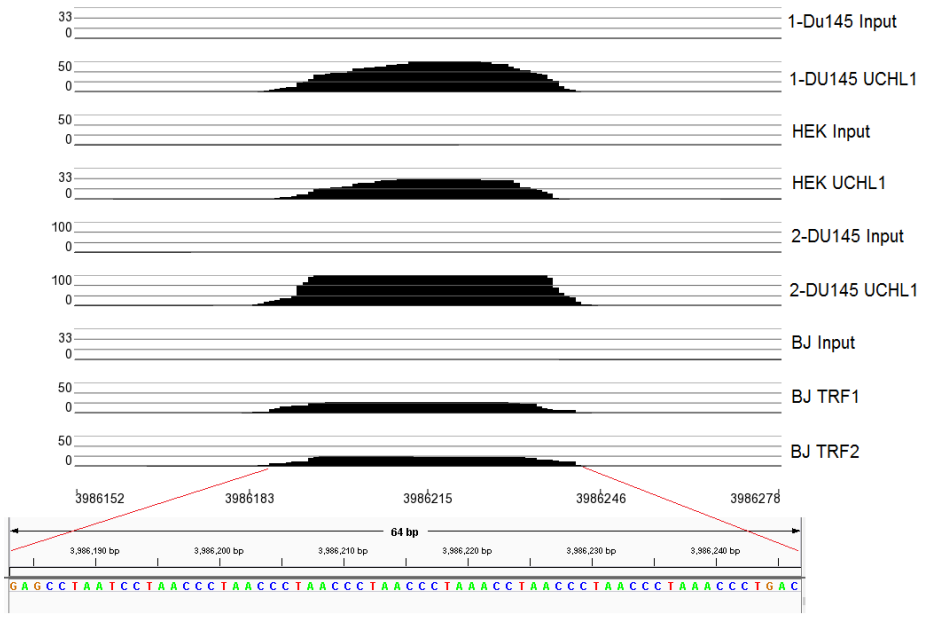

D

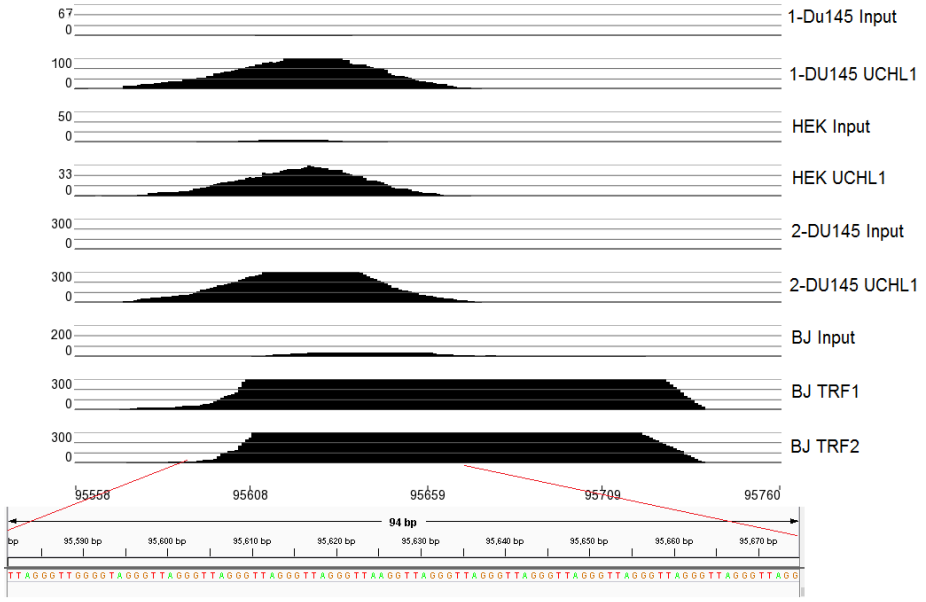

Figure 17. Alignment of input and UCHL1 ChIP-seq peaks from DU145 formaldehyde only cross-linked cells (1-DU145), dual cross-linked HEK293T (HEK) and DU145 (2-DU145) cells along with the Simonet *et al.,* 2011 raw data from input BJ cells, TRF1 and TRF2 (BJ TRF1/2) ChIP-seq. The ChIP-seq peaks co-localize to the intronic regions of the *CLIC6* (A) and *FAM157A* (B) and distal intergenic regions of chromosomes 10 (C) and 12 (D).

Also, there were instances where UCHL1 did not co-localize to the same genomic locations as TRF1 and TRF2 (Figure 17). However, it is important to note that the TRF1 and TRF2 peak data was obtained from a study with transformed BJ fibroblast cells. Examples include a peak in the intronic region of the *LRP1B* gene on chromosome 2 (Figure 17A) and also in the intronic region of the *PLXNB2* gene on chromosome 22 (Figure 17B). The opposite was also observed where TRF1 and TRF2 peaks were not observed at the same genomic locations of UCHL1 peaks (Figure 18). These examples, however, were not as common as matching UCHL1 and TRF1/2 peaks. Examples include a peak in the intronic region of the *CHRDL2* gene on chromosome 11 (Figure 18A) and also in the intergenic region of chromosome 18 (Figure 18B).

A

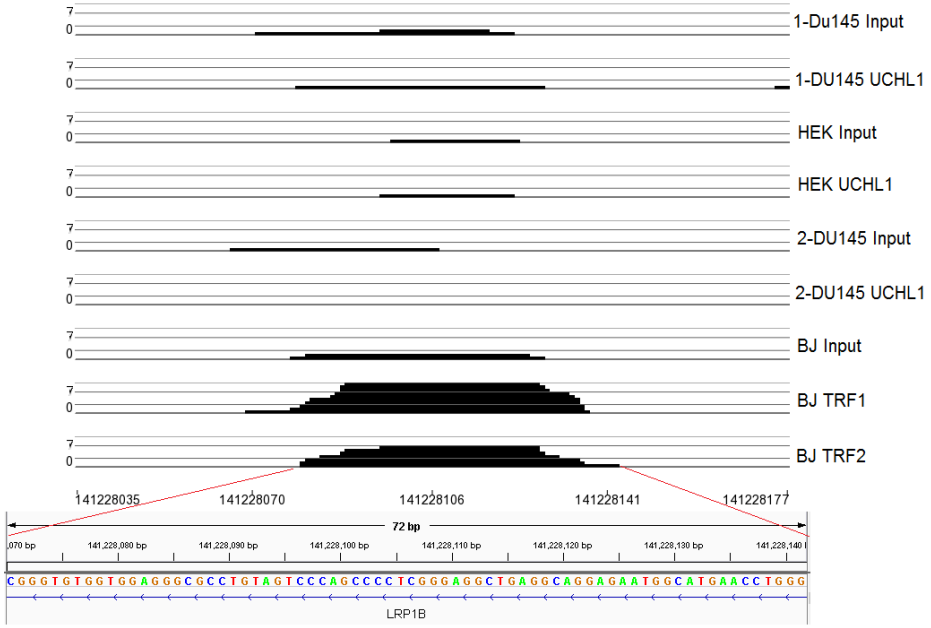

B

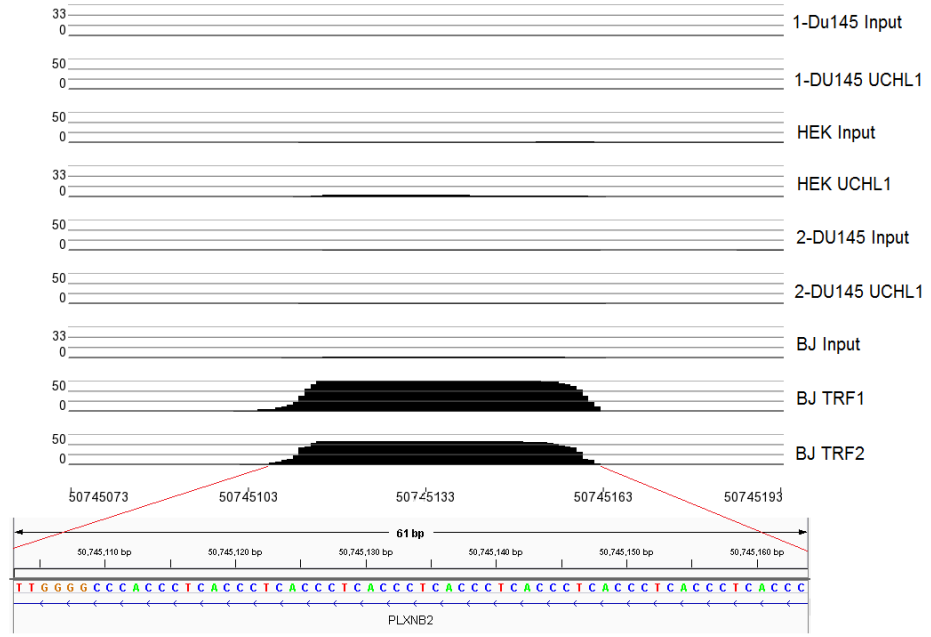

Figure 18. Alignment of input and UCHL1 ChIP-seq peaks from DU145 formaldehyde only cross-linked cells (1-DU145), dual cross-linked HEK293T (HEK) and DU145 (2-DU145) cells along with the Simonet *et al.,* 2011 raw data from input BJ cells, TRF1 and TRF2 (BJ TRF1/2) ChIP-seq. The UCHL1 ChIP-seq peaks do not co-localize with TRF1/2 at the intronic regions of the *LRP1B* (A) and *PLXNB2* (B) genes.

A

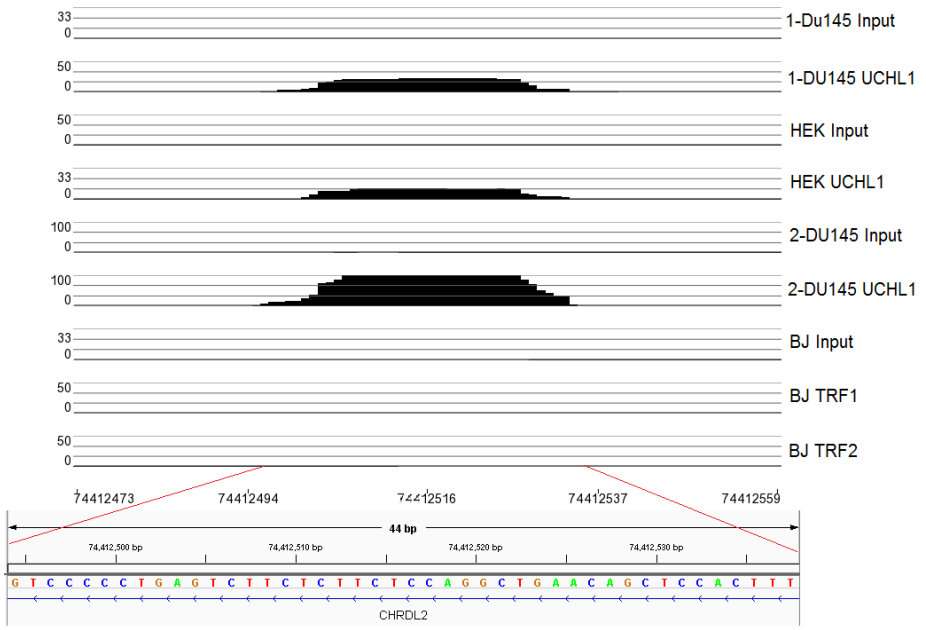

B

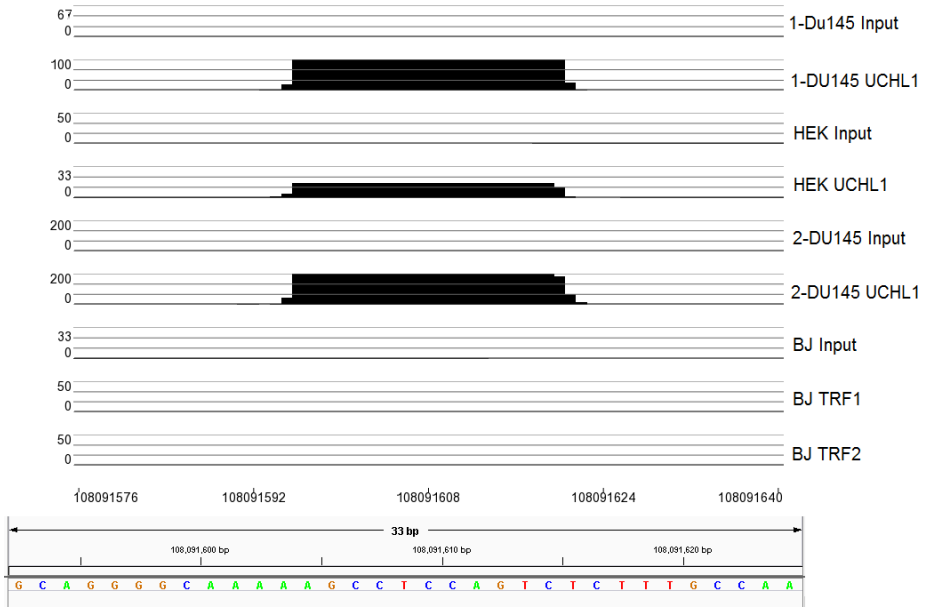

Figure 19. Alignment of input and UCHL1 ChIP-seq peaks from DU145 formaldehyde only cross-linked cells (1-DU145), dual cross-linked HEK293T (HEK) and DU145 (2-DU145) cells along with the Simonet *et al.,* 2011 raw data from input BJ cells, TRF1 and TRF2 (BJ TRF1/2) ChIP-seq. The TRF1/2 ChIP-seq peaks did not co-localize with UCHL1 at the intronic region of the *CHRDL2* gene (A) and at the intergenic region of chromosome 18 (B).

Chapter 5: Discussion

UCHL1 was not shown to bind to the regulatory regions of pro- or anti-apoptotic genes or genes involved in the cell cycle. Thus, UCHL1 likely does not regulate these genes by its association with regulatory regions and further analyses are need to determine whether UCHL1 has a role in gene expression as it was hypothesized in this study. However, UCHL1 was shown to potentially associate and co-localize to the DNA with the shelterin complex, which makes this an exciting new discovery.

5.1 UCHL1 Expression and Association with DNA

UCHL1 was only expressed in DU145 but not in other prostate cancer cells in this study. The DU145 prostate cancer cell line was derived from the central nervous system (brain) metastasis site of a 69-year-old male (Stone *et al.,* 1978). It is unclear why UCHL1 is only expressed in this particular cell line. One reason is possibly the fact that UCHL1 is a very abundant neuronal protein and DU145 being derived from the brain (Stone *et al.,* 1978; Day and Thompson, 2010). Since UCHL1 was derived from this physiological environment, it would be reasonable to speculate UCHL1 expression is dependent on the environment the cell line was derived from. Also, it is suggested that UCHL1 is a marker for neuroendocrine cells. It is believed that UCHL1 expression in DU145 cells demonstrates that these cells have potentially undergone the process of neuroendocrine differentiation (Leiblich *et al.,* 2007).

Others have suggested that UCHL1 is likely an oncogene involved in cancer pathogenesis and progression that promotes metastasis (Hurst-Kennedy *et al.,* 2012).

Thus, UCHL1 is expressed in metastatic cancer cell lines like DU145. One study demonstrated that UCHL1 interacts and stabilizes β-catenin. This leads to β-catenin regulated gene expression of oncogenes such as *C-MYC* and *SURVIVIN* (Bheda *et al.,* 2009a). A study by Jang *et al.,* 2011 showed that UCHL1 overexpression in benign prostate tumour cells led to epithelial-to-mesenchymal transition (EMT), which in turn led to increased cancer cell invasion metastasis. Similarly, knockdown of UCHL1 in DU145 cells led to MET (opposite of EMT) and resulted in decreased cell invasiveness and migration (Jang *et al.,* 2011). This suggests that UCHL1 expression in metastatic prostate cancer cells is due to the role UCHL1 has in cancer invasiveness and migration.

To date, the UCHL1 association with DNA has never been reported. In this study, it was also demonstrated that the UCHL1 interaction with DNA is most likely indirect, i.e. UCHL1 interacts with another protein that is bound to DNA. Interestingly, other proteins from the UCH subclass have been shown to be associated with chromatin. These include UCHL5 and BAP1. UCHL5 is associated with chromatin but does not deubiquitinate histones. It has a distinct function even independent of its role on the 19S proteasome. In the nucleus, UCHL5 is associated with the human Ino80 chromatin-remodelling complex, hINO80. This suggests that UCHL5 and hINO80 are potentially involved in the regulation of gene expression (Yao *et al.,* 2008). BAP1 is another example of an UCH that is associated with chromatin as a part of the PR-DUB complex and through the interaction with HCF-1. BAP1 interacts with HCF-1 (host cell factor 1) and deubiquitinates HCF-1 (Misaghi *et al.,* 2009). HCF-1 is a transcriptional regulator of gene promoters that are associated E2F transcriptional factors. E2F transcription factors play a role in recruitment of histone methyltransferases, which results in expression of

genes required for G1/S cell cycle progression (Tyagi *et al.,* 2007). This suggests that BAP1 has a role in regulating the cell cycle and proliferation by deubiquitinating HCF-1 (Machida *et al.,* 2009). BAP1 is also a part of the PR-DUB (polycomb repressive-deubiquitinase) complex. BAP1 interaction with ASXL1 PcG protein results in the formation of the PR-DUB complex. This complex regulates histone H2A deubiquitination and suppression of the *HOX* gene (Scheuermann *et al.,* 2010). Since this is the case with structurally similar proteins from the UCH subclass, it might not be surprising that UCHL1 is associated with DNA. Also, it is important to note that the UCHL1 function in relation to DNA could potentially be DUB independent.

5.2 UCHL1 Repressions and Treatment with Epigenetic Drugs

Previous studies have shown that UCHL1 expression is suppressed by promoter methylation in some prostate cancer tumour samples as well as in LNCaP and PC3 cells. Mitsui *et al.,* 2012 reported that 37 out of 226 prostate cancer tissues examined had methylated UCHL1 promoters. It was also demonstrated that treatment of the LNCaP and PC3 prostate cancer cells with the DNA methyltransferase 1 inhibitor, 5-aza-2′-deoxycytidine, induces the expression of UCHL1 mRNA in both or just in LNCaP and not PC3 prostate cancer cell lines proving to be inconsistent (Mitsui *et al.,* 2012; Tokumaru *et al.,* 2008). Mitsui *et al.,* 2012 induced UCHL1 mRNA expression in both LNCaP and PC3 prostate cancer cells. Tokumaru *et al.,* 2008 claim UCHL1 mRNA expression was induced in LNCaP but not in PC3 prostate cancer cells. However, the actual figure of an agarose gel from Tokumaru *et al.,* 2008 shows very little or no induction and is inconclusive whether UCHL1 was induced (Tokumaru *et al.,* 2008).

Also, these studies have not shown whether the UCHL1 protein expression is induced after 5-aza-2′-deoxycytidine treatment, which was essential for Aim 1 in this study. After repeating these treatments, UCHL1 mRNA and protein were not induced. The repressive complex comprised of DNA methyltransferase 1, histone deacetylases (HDACs) and PcG proteins have previously been shown to silence certain tumour suppressor genes (Tsai and Baylin 2011). Therefore, the prostate cancer cell lines were treated with a combination of 5-aza-2′-deoxycytidine and a HDAC inhibitor TSA, as it has been previously described (Walton *et al.,* 2008). Again, this treatment produced identical results to the initial 5-aza-2′-deoxycytidine treatment, where UCHL1 mRNA and protein were only expressed in DU145 but not in LNCaP, PC3 and C4-2 prostate cancer cells.

Tokumaru *et al.,* 2008 showed that in some cases UCHL1 was not always induced after treatment with 5-aza-2′-deoxycytidine. For example, UCHL1 mRNA was not induced in PC3 prostate cancer cells, HTB3 and HTB4 bladder cancer cells or HT29 colorectal cancer cells (Tokumaru *et al.,* 2008). It is also questionable whether UCHL1 expression was induced in LNCaP cells (Tokumaru *et al.,* 2008).

It was thus conceivable that the UCHL1 gene was mutated or deleted in PC3, LNCaP and C4-2 prostate cancer cell lines and thus not epigenetically silenced. A useful bioinformatic tool called Cancer Cell Line Encyclopaedia (CCLE) from the Broad and Novaris Institutes allows access to genomic information from approximately 1000 cancer cell lines (http://www.broadinstitute.org/ccle/home). This includes specific gene variants such as mutations and deletions. Data from the CCLE suggests that the UCHL1 gene is not deleted or mutated in LNCaP and PC3 prostate cancer cells. This means that UCHL1 is likely epigenetically silenced by a possible mechanism independent of or in addition to

DNA methylation and histone deacetylation. One possibility is that UCHL1 is epigenetically silenced by histone methylation; examples include H3K9me3 and H3K27me3 that result in transcriptional silencing. Another possibility could be transcription factors involved in the regulation of UCHL1 gene expression.

5.3 UCHL1 and Transcription Factor p53

The interaction between UCHL1 and p53 was reported in two separate studies. This was the case in UCHL1 overexpressed nasopharyngeal cancer cell lines and UCHL1 transfected HCT116 colorectal cancer cell line. UCHL1 and p53 also interact in HEK293T cells, where UCHL1 and p53 are endogenously expressed (Li *et al.,* 2010; Yu *et al.,* 2008). Both studies have proposed an identical model for the interaction, where UCHL1 is a tumour suppressor that deubiquitinates p53 leading to its stabilization and activation. This results in downstream pathways that lead to apoptosis and cell cycle arrest. It is also proposed that the UCHL1 ligase function may also play a role in the ubiquitination of the p53 negative regulator MDM2 (Li *et al.,* 2010). Another study by Ummanni *et al.,* 2011 demonstrated that overexpression of UCHL1 in LNCaP prostate cancer cells leads to increased protein expression of p53 and $p14^{ARF}$ and decreased levels of the p53 negative regulator MDM2, suggesting that UCHL1 is a tumour suppressor that suppresses cell proliferation and anchorage-independent growth. On the other hand, UCHL1 knockdown studies in HEK293T cells show an increase in several genes regulated by p53 that play a role in apoptosis and cell cycle arrest, suggesting that UCHL1 is an oncogene that promotes p53 degradation by poly-ubiquitination (Bheda *et al.,* 2009b).

In this study, it was demonstrated that the UCHL1 and p53 interaction was also evident in DU145 prostate cancer cells. The UCHL1 knockdown study by Bheda *et al.,* 2009b suggests that UCHL1 regulates the upregulation of pro-apoptotic and down-regulation of anti-apoptotic genes. Since the expression of several of these genes is directly regulated by p53, ChIP analyses were performed to show if UCHL1 and p53 co-localize to the regulatory regions of specific genes. Two genes regulated by p53 were chosen for this study, *CDKN1A* and *BAX*. However, qPCR analyses with ChIP DNA did not show enrichment at p53 binding sites on the *CDKN1A* and *BAX* upstream promoter regions. Literature searches show that investigators usually study p53 DNA binding under stress conditions by stimulating the cells with agents such as UV light or 5-fluorouracil (Kaeser *et al.,* 2004). During this study, UCHL1 was shown to be cross-linked to DNA under normal unstimulated physiological conditions. Also, it was reported that DU145 cells have a p53 heterozygous mutant (P223L and V274F) (Isaacs *et al.,* 1991). Both of these mutations are located within the p53 DNA binding domain. However, CCLE data suggest that the DU145 p53 mutation is found in only one allele, V274F. Moreover, Bajgelman and Strauss, 2006 have suggested that the P223L p53 mutation is temperature sensitive in DU145 cells. p53 target gene activation was observed at 37°C and 32°C where some target genes were induced at 32°C (Bajgelman and Strauss, 2006). Additionally, the HEK293T cell line contains the SV40 large T antigen that in fact inhibits p53 activity (Ahuja *et al.,* 2005; DuBridge *et al.,* 1987). It can be concluded that p53 DNA binding may be affected and considerably reduced due to these reasons. Therefore, it was decided to not pursue p53 targets further but rather focus on the unbiased screening approach, ChIP-seq.

Bheda *et al.,* 2009b UCHL1 knockdown study proposed that UCHL1 has a role in the expression of pro- and anti-apoptotic genes as well as genes involved in the regulation of the cell cycle. The fact that UCHL1 regulates the expression of these genes can potentially be explained by its interaction with multiple CDKs. CDKs are vital in cell cycle regulation and cell proliferation due to their kinase activity and phosphorylation of target proteins involved in the cell cycle. A recent study by Kabuta *et al.,* 2013 showed that UCHL1 interacts with CDK1, CDK4, CDK5 and CDK6. It is believed that UCHL1 enhances the kinase activity of the CDKs. Also, the interaction between CDKs and UCHL1 was independent of UCHL1 DUB activity meaning UCHL1 does not deubiquitinate the CDKs in order to enhance their kinase activity. It was also demonstrated that UCHL1 overexpression in HeLa cells, which do not express UCHL1, resulted in an increase in cell proliferation. Similarly, UCHL1 knockdown in UCHL1 expressing cells resulted in a decrease of cell proliferation (Kabuta *et al.,* 2013). This suggests that UCHL1 is a vital regulator of CDKs and consequently an important factor in cell cycle regulation.

5.4 UCHL1 and the Shelterin Complex

Due to the Bheda *et al.,* 2009b UCHL1 knockdown study, it was hypothesized that UCHL1 has a role in the expression of pro- and anti-apoptotic genes as well as genes involved in the regulation of the cell cycle. The potential that UCHL1 is associated and co-localizes to the DNA with the shelterin complex is an exciting new discovery, which will require further investigation to elucidate the functional role of UCHL1.

To the best of our knowledge, only Lee *et al.,* 2011 have provided evidence for an interaction between UCHL1 and two shelterin proteins, RAP1 and TIN2. In this study, the investigators identified over 300 proteins that were associated with at least one of the six shelterin complex proteins. The authors used the yellow fluorescent protein-based protein complementation assay and also validated by co-precipitation by glutathione S-transferase (GST) pull-down (Lee *et al.,* 2011). However, since this was a genome-wide analysis the interaction between UCHL1 and the shelterin proteins RAP1 and TIN2 was not further investigated.

UCHL1 and multiple TRF1 and TRF2 target sites are located at telomeres or at ITSs. Many of these target sites are located within the gene body of various genes. Examples of target sites within genes from Section 4.4.3 include *CLIC6* and *FAM157A* where UCHL1, TRF1 and TRF2 co-localize; *LRP1B* and *PLXNB2* genes where only TRF1 and TRF2 co-localize; and UCHL1 only target gene *CHRDL2*. It is important to note that the TRF1 and TRF2 peak data was obtained from a study with transformed BJ fibroblast cells, whereas the UCHL1 peaks were from DU145 or HEK293T cells. This fact could also play a role in whether UCHL1/TRF1/TRF2 bind to the gene body of the genes mentioned.

To identify whether UCHL1/TRF1/TRF2 binding affects gene expression of genes these proteins bind to, RNA-seq data from DU145 and HEK293T cells would have to be analyzed. However, this RNA-seq data was not available but by using ChIP-seq data available from the ENCODE database (http://genome.ucsc.edu/ENCODE), it is possible to look at epigenetic marks from HEK293 cells and determine whether binding of UCHL1, TRF1 and TRF2 to the gene body affects gene expression. HEK293T cells

used for UCHL1 ChIP-seq are a variant cell line of HEK293 and contain the SV40 Large T-antigen (DuBridge *et al.,* 1987). The H3K4me3 is a marker for active/poised chromatin and an H3K4me3 peak at the 5'-end of a gene can be used as a marker for gene expression. The *CLIC6, LRP1B, PLXNB2* and *CHRDL2* are all protein-coding genes, while *FAM157A* is a RNA gene part of the long non-coding RNA (lncRNA) family. By analyzing the HEK293 ENCODE data, it is evident that all of the protein-coding genes contain an H3K4me3 peak at the gene 5'-ends, while *FAM157A* does not. It appears that UCHL1, TRF1 and TRF2 co-localization, UCHL1 only or no UCHL1 binding does not play a role in the expression of these particular genes as these genes are all expressed independent of UCHL1, TRF1 and TRF2 binding in the gene body.

The reason why ITSs are found in intrachromosomal sites and within gene bodies is not entirely understood. As previously mentioned, it is believed that ITSs were generated through evolutionary chromosomal rearrangements such as chromosomal fusions and inversions. Also, ITSs are prone to chromosomal rearrangements, recombination, breakage and amplification (Lin and Yan, 2008). Kilburn *et al.,* 2001 reported that ITSs within a gene intron cause chromosome instability (Kilburn *et al.,* 2001). During this study, the investigators inserted an 800 bp telomeric repeat (TTAGGG) into an intron of the *APRT* gene in Chinese hamster ovary cells. The insertion did not affect the expression of the *APRT* gene. However, there was a 30-fold increase in gene rearrangement and thus chromosomal instability. Therefore, the shelterin complex may potentially play an important role in maintaining the stability of ITSs. In cancer, some ITSs correspond to cancer fragile sites where chromosomal breakage occurs by mutagens or carcinogens resulting in cancer pathogenesis (Lin and Yan, 2008).

The role of UCHL1 with the shelterin complex can at this time only be speculated. One theory is that UCHL1 may simply ubiquitinate or deubiquitinate shelterin proteins through its ligase or DUB activity, respectively. A study by Chang *et al.,* 2003 showed that TRF1 of the shelterin complex is ubiquitinated and degraded once it is released from the telomere. TRF1 is only ubiquitinated when it is not bound to telomeres (Chang *et al.,* 2003). It has also been shown that as part of the SAGA complex, DUB USP22 deubiquitinates TRF1 resulting in binding to telomeric repeats (Atanassov *et al.,* 2009). If UCHL1 associated with the shelterin proteins has DUB or ligase activity, this would suggest that UCHL1 plays a role in the protein turnover of the shelterin complex.

Another hypothesis is that UCHL1 plays a role in anchoring the shelterin complex to the nuclear matrix structure. Previous data from the Davie lab has shown that isolated nuclear matrix proteins and cisplatin DNA cross-linked proteins have almost identical 2D gel patterns (Samuel *et al.,* 1998). This would mean that cisplatin cross-linking and isolation of cross-linked proteins could be used as a method to isolate nuclear matrix proteins. Since UCHL1 is a protein readily cross-linked to DNA by cisplatin, it can be assumed that UCHL1 is a nuclear matrix protein. UCHL1 interacting protein TIN2 of the shelterin complex has recently been associated with the nuclear matrix. An isoform of TIN2 was identified as a protein that tethers telomeres to the nuclear matrix (Kaminker *et al.,* 2009). Another UCHL1 interacting protein, RAP1, has been associated with the nuclear envelope. During postmitotic nuclear assembly, telomeres localize to the nuclear envelope through the interaction between RAP1 and nuclear envelope protein Sun1 (Crabbe *et al.,* 2012). Also, a methylated form of the TRF2 shelterin protein has recently

been shown to be associated with the nuclear matrix (Mitchell and Zhu, 2014). Since this is the case, it is possible that UCHL1 also has a role in tethering the shelterin complex along with telomeres and ITSs to the nuclear matrix, regulating the organization of chromatin.

5.5 Conclusions and Significance

The exact function of UCHL1 is still unclear and disputed. It is almost certain that UCHL1 is a multifunctional protein involved in several cellular processes. These include deubiquitination, ubiquitination, ubiquitin homeostasis and enhancing CDK activity. Thus it is not unusual to suspect that there are other cellular functions of UCHL1 that may be independent of its DUB or ligase activity. Further research is needed to investigate the exact role UCHL1 has in association with the shelterin complex. Moreover, the association of UCHL1 and the shelterin complex may shed light on the role that UCHL1 has in certain metastatic cancers and in neurodegenerative diseases such as Parkinson's disease. It has been shown that UCHL1^{I93M} mutation results in a 50% decrease of catalytic activity Parkinson's disease. Therefore, it is important to investigate whether this particular mutation affects the association with the shelterin complex.

5.6 Future Directions

To further investigate the UCHL1 association with the shelterin complex, several experiments are proposed. Firstly, Co-IP experiments are vital to confirm that UCHL1 in fact interacts with proteins of the shelterin complex in DU145 and HEK293T cells. It is likely that the whole shelterin complex will be immunoprecipitated, hence it will be

difficult to determine the exact shelterin protein UCHL1 interacts with but rather if UCHL1 interacts with the entire complex. Co-IP experiments will be done with both UCHL1 antibodies as well as commercially available immunoprecipitation antibodies for shelterin proteins such as TRF1, TRF2 and RAP1. Secondly, immunofluorescence (IF) experiments will confirm whether UCHL1 co-localizes with shelterin proteins such as TRF1, TRF2 and RAP1. Additionally, IF will determine the chromosomal regions of co-localization, such as telomeres or ITSs.

The validity of the ChIP-seq results will be confirmed with ChIP assays. ChIP assays will be performed by isolating UCHL1 ChIP DNA and interrogating the UCHL1 bound DNA with primers placed on either side of UCHL1 target sites. In the past, this has presented difficulty due to the repetitive nature of the target sites. However, studies by Yang *et al.,* 2011 and Simonet *et al.,* 2011 have demonstrated that in fact it is possible to validate some of the ChIP-seq targets. Since multiple ChIP-seq peaks from these studies match with the UCHL1 ChIP-seq peaks, it is possible to use the same primer sequences in the validation of UCHL1 ChIP-seq data.

UCHL1 knockdown studies will further investigate its role in regards to the shelterin complex. Knocking down UCHL1 will allow us to investigate, by western blot analyses, if UCHL1 affects the expression of the shelterin proteins. Also, ChIP experiments with shelterin proteins TRF1 or TRF2 in cells where UCHL1 is knocked down will determine whether UCHL1 plays a role in the shelterin complex binding to specific DNA targets. If the shelterin complex does not bind to validated genomic locations once UCHL1 is knocked down, it will be clear that UCHL1 plays a role in shelterin DNA binding. Additionally, by checking the expression of UCHL1 target genes

before and after UCHL1 knockdown will determine whether UCHL1 in fact plays a role in gene expression of these target genes.

Furthermore, site-directed mutagenesis experiments as in Kabuta *et al.,* 2013 will be performed to generate an $UCHL1^{C90S}$ mutant that does not posses DUB or ligase activity. This will confirm whether the UCHL1 role with the shelterin complex is dependent on DUB or ligase activity as well as whether binding to the nuclear matrix is DUB or ligase activity dependent.

Chapter 6: References

Abrahamsson, P. A. (2010). Potential benefits of intermittent androgen suppression therapy in the treatment of prostate cancer: a systematic review of the literature. *European urology*, *57*(1), 49-59.

Aguilar, R. C., & Wendland, B. (2003). Ubiquitin: not just for proteasomes anymore. *Current opinion in cell biology*, *15*(2), 184-190.

Ahuja, D., Sáenz-Robles, M. T., & Pipas, J. M. (2005). SV40 large T antigen targets multiple cellular pathways to elicit cellular transformation. *Oncogene*, *24*(52), 7729-7745.

Akishima-Fukasawa, Y., Ino, Y., Nakanishi, Y., Miura, A., Moriya, Y., Kondo, T., ... & Hirohashi, S. (2010). Significance of PGP9. 5 expression in cancer-associated fibroblasts for prognosis of colorectal carcinoma. *American journal of clinical pathology*, *134*(1), 71-79.

Amerik, A. Y., & Hochstrasser, M. (2004). Mechanism and function of deubiquitinating enzymes. *Biochimica et Biophysica Acta (BBA)-Molecular Cell Research*, *1695*(1), 189-207.

Atanassov, B. S., Evrard, Y. A., Multani, A. S., Zhang, Z., Tora, L., Devys, D., ... & Dent, S. Y. (2009). Gcn5 and SAGA regulate shelterin protein turnover and telomere maintenance. *Molecular cell*, *35*(3), 352-364.

Azzalin, C. M., Nergadze, S. G., & Giulotto, E. (2001). Human intrachromosomal telomeric-like repeats: sequence organization and mechanisms of origin. *Chromosoma*, *110*(2), 75-82.

Bajgelman, M. C., & Strauss, B. E. (2006). The DU145 human prostate carcinoma cell line harbors a temperature-sensitive allele of p53. *The Prostate*, *66*(13), 1455-1462.

Balk, S. P., Ko, Y. J., & Bubley, G. J. (2003). Biology of prostate-specific antigen. *Journal of Clinical Oncology*, *21*(2), 383-391.

Baumeister, W., Walz, J., Zühl, F., & Seemüller, E. (1998). The proteasome: paradigm of a self-compartmentalizing protease. *Cell*, *92*(3), 367-380.

Beckerman, R., & Prives, C. (2010). Transcriptional regulation by p53. *Cold Spring Harbor perspectives in biology*, *2*(8), a000935.

Berger, S. L. (2007). The complex language of chromatin regulation during transcription. *Nature*, *447*(7143), 407-412.

Bheda, A., Shackelford, J., & Pagano, J. S. (2009b). Expression and functional studies of ubiquitin C-terminal hydrolase L1 regulated genes. *PLoS One*, *4*(8), e6764.

Bheda, A., Yue, W., Gullapalli, A., Whitehurst, C., Liu, R., Pagano, J. S., & Shackelford, J. (2009a). Positive reciprocal regulation of ubiquitin C-terminal hydrolase L1 and β-catenin/TCF signaling. *PLoS One*, *4*(6), e5955.

Blackburn, E. H., & Gall, J. G. (1978). A tandemly repeated sequence at the termini of the extrachromosomal ribosomal RNA genes in Tetrahymena. *Journal of molecular biology*, *120*(1), 33-53.

Boyd, L. K., Mao, X., & Lu, Y. J. (2012). The complexity of prostate cancer: genomic alterations and heterogeneity. *Nature Reviews Urology*, *9*(11), 652-664.

Caballero, O. L., Resto, V., Patturajan, M., Meerzaman, D., Guo, M. Z., Engles, J., ... & Jen, J. (2002). Interaction and colocalization of PGP9. 5 with JAB1 and p27 (Kip1). *Oncogene*, *21*(19), 3003-3010.

Cao, J., & Yan, Q. (2012). Histone ubiquitination and deubiquitination in transcription, DNA damage response, and cancer. *Frontiers in oncology*, *2*.

Chai, W., Shay, J. W., & Wright, W. E. (2005). Human telomeres maintain their overhang length at senescence. *Molecular and cellular biology*, *25*(6), 2158-2168.

Chang, W., Dynek, J. N., & Smith, S. (2003). TRF1 is degraded by ubiquitin-mediated proteolysis after release from telomeres. *Genes & development*, *17*(11), 1328-1333.

Chen, G., Gharib, T. G., Huang, C. C., Thomas, D. G., Shedden, K. A., Taylor, J. M., ... & Beer, D. G. (2002). Proteomic analysis of lung adenocarcinoma identification of a highly expressed set of proteins in tumors. *Clinical Cancer Research*, *8*(7), 2298-2305.

Chiam, K., Centenera, M. M., Butler, L. M., Tilley, W. D., & Bianco-Miotto, T. (2011). GSTP1 DNA methylation and expression status is indicative of 5-aza-2′-deoxycytidine efficacy in human prostate cancer cells. *PLoS One*, *6*(9), e25634.

Choi, J., Levey, A. I., Weintraub, S. T., Rees, H. D., Gearing, M., Chin, L. S., & Li, L. (2004). Oxidative modifications and down-regulation of ubiquitin carboxyl-terminal hydrolase L1 associated with idiopathic Parkinson's and Alzheimer's diseases. *Journal of Biological Chemistry*, *279*(13), 13256-13264.

Collas, P. (2010). The current state of chromatin immunoprecipitation. *Molecular biotechnology*, *45*(1), 87-100.

Crabbe, L., Cesare, A. J., Kasuboski, J. M., Fitzpatrick, J. A., & Karlseder, J. (2012). Human telomeres are tethered to the nuclear envelope during postmitotic nuclear assembly. *Cell reports*, *2*(6), 1521-1529.

Culig, Z., Hobisch, A., Hittmair, A., Peterziel, H., Cato, A. C., Bartsch, G., & Klocker, H. (1998). Expression, structure, and function of androgen receptor in advanced prostatic carcinoma. *The Prostate*, *35*(1), 63-70.

Das, C., Hoang, Q. Q., Kreinbring, C. A., Luchansky, S. J., Meray, R. K., Ray, S. S., ... & Petsko, G. A. (2006). Structural basis for conformational plasticity of the Parkinson's disease-associated ubiquitin hydrolase UCH-L1. *Proceedings of the National Academy of Sciences of the United States of America*, *103*(12), 4675-4680.

Day, I. N., & Thompson, R. J. (2010). UCHL1 (PGP 9.5): neuronal biomarker and ubiquitin system protein. *Progress in neurobiology*, *90*(3), 327-362.

De Lange, T. (2005). Shelterin: the protein complex that shapes and safeguards human telomeres. *Genes & development*, *19*(18), 2100-2110.

Delcuve, G. P., Rastegar, M., & Davie, J. R. (2009). Epigenetic control. *Journal of cellular physiology*, *219*(2), 243-250.

Dennissen, F. J., Kholod, N., Hermes, D. J., Kemmerling, N., Steinbusch, H. W., Dantuma, N. P., & van Leeuwen, F. W. (2011). Mutant ubiquitin (UBB+1) associated with neurodegenerative disorders is hydrolyzed by ubiquitin C-terminal hydrolase L3 (UCH-L3). *FEBS letters*, *585*(16), 2568-2574.

Diotti, R., & Loayza, D. (2011). Shelterin complex and associated factors at human telomeres. *Nucleus*, *2*(2), 119-135.

Doran, J. F., Jackson, P., Kynoch, P. A., & Thompson, R. J. (1983). Isolation of PGP 9.5, a New Human Neurone-Specific Protein Detected by High-Resolution Two-Dimensional Electrophoresis. *Journal of neurochemistry*, *40*(6), 1542-1547.

DuBridge, R. B., Tang, P., Hsia, H. C., Leong, P. M., Miller, J. H., & Calos, M. P. (1987). Analysis of mutation in human cells by using an Epstein-Barr virus shuttle system. *Molecular and cellular biology*, *7*(1), 379-387.

Eletr, Z. M., & Wilkinson, K. D. (2011). An emerging model for BAP1's role in regulating cell cycle progression. *Cell biochemistry and biophysics*, *60*(1-2), 3-11.

Fang, Y., Fu, D., & Shen, X. Z. (2010). The potential role of ubiquitin c-terminal hydrolases in oncogenesis. *Biochimica et Biophysica Acta (BBA)-Reviews on Cancer*, *1806*(1), 1-6.

Friesen, C., Herr, I., Krammer, P. H., & Debatin, K. M. (1996). Involvement of the CD95 (APO–1/Fas) receptor/ligand system in drug–induced apoptosis in leukemia cells. *Nature medicine*, *2*(5), 574-577.

Gilmour, D. S., & Lis, J. T. (1985). In vivo interactions of RNA polymerase II with genes of Drosophila melanogaster. *Molecular and cellular biology*, *5*(8), 2009-2018.

Hamazaki, J., Iemura, S. I., Natsume, T., Yashiroda, H., Tanaka, K., & Murata, S. (2006). A novel proteasome interacting protein recruits the deubiquitinating enzyme UCH37 to 26S proteasomes. *The EMBO journal*, *25*(19), 4524-4536.

Hanaoka, S., Nagadoi, A., Yoshimura, S., Aimoto, S., Li, B., de Lange, T., & Nishimura, Y. (2001). NMR structure of the hRap1 Myb motif reveals a canonical three-helix bundle lacking the positive surface charge typical of Myb DNA-binding domains. *Journal of molecular biology*, *312*(1), 167-175.

Healy, D. G., Abou-Sleiman, P. M., Casas, J. P., Ahmadi, K. R., Lynch, T., Gandhi, S., ... & Wood, N. W. (2006). UCHL-1 is not a Parkinson's disease susceptibility gene. *Annals of neurology*, *59*(4), 627-633.

Hershko, A. & Ciechanover, A. (1998). The ubiquitin system. *Annu Rev Biochem*, *67*, 425-479.

Horoszewicz, J. S., Leong, S. S., Chu, T. M., Wajsman, Z. L., Friedman, M., Papsidero, L., ... & Sandberg, A. A. (1980). The LNCaP cell line--a new model for studies on human prostatic carcinoma. *Progress in clinical and biological research*, *37*, 115.

Hurst-Kennedy, J., Chin, L. S., & Li, L. (2012). Ubiquitin C-terminal hydrolase l1 in tumorigenesis. *Biochemistry research international*, *2012*.

Husnjak, K., & Dikic, I. (2012). Ubiquitin-binding proteins: decoders of ubiquitin-mediated cellular functions. *Annual review of biochemistry*, *81*, 291-322.

Isaacs, W. B., Carter, B. S., & Ewing, C. M. (1991). Wild-type p53 suppresses growth of human prostate cancer cells containing mutant p53 alleles. *Cancer research*, *51*(17), 4716-4720.

Jang, M. J., Baek, S. H., & Kim, J. H. (2011). UCH-L1 promotes cancer metastasis in prostate cancer cells through EMT induction. *Cancer letters*, *302*(2), 128-135.

Jemal, A., Bray, F., Center, M. M., Ferlay, J., Ward, E., & Forman, D. (2011). Global cancer statistics. *CA: a cancer journal for clinicians*, *61*(2), 69-90.

Jensen, D. E., Proctor, M., Marquis, S. T., Gardner, H. P., Ha, S. I., Chodosh, L. A., ... & Rauscher 3rd, F. J. (1998). BAP1: a novel ubiquitin hydrolase which binds to the BRCA1 RING finger and enhances BRCA1-mediated cell growth suppression. *Oncogene*, *16*(9), 1097-1112.

Kabuta, T., Mitsui, T., Takahashi, M., Fujiwara, Y., Kabuta, C., Konya, C., ... & Wada, K. (2013). Ubiquitin C-terminal Hydrolase L1 (UCH-L1) Acts as a Novel Potentiator of Cyclin-dependent Kinases to Enhance Cell Proliferation Independently of Its Hydrolase Activity. *Journal of Biological Chemistry*, *288*(18), 12615-12626.

Kaeser MD, Pebernard S, Iggo RD (2004) Regulation of p53 stability and function in HCT116 colon cancer cells. *J Biol Chem.* 279(9):7598-605.

Kaighn, M. E., Narayan, K. S., Ohnuki, Y., Lechner, J. F., & Jones, L. W. (1979). Establishment and characterization of a human prostatic carcinoma cell line (PC-3). *Investigative urology*, *17*(1), 16-23.

Kaminker, P. G., Kim, S. H., Desprez, P. Y., & Campisi, J. (2009). A novel form of the telomere-associated protein TIN2 localizes to the nuclear matrix. *Cell Cycle*, *8*(6), 931-939.

Kilburn, A. E., Shea, M. J., Sargent, R. G., & Wilson, J. H. (2001). Insertion of a telomere repeat sequence into a mammalian gene causes chromosome instability. *Molecular and cellular biology*, *21*(1), 126-135.

Kim, J. H., Park, K. C., Chung, S. S., Bang, O., & Chung, C. H. (2003). Deubiquitinating enzymes as cellular regulators. *Journal of biochemistry*, *134*(1), 9-18.

Kinoshita, H., Shi, Y., Sandefur, C., Meisner, L. F., Chang, C., Choon, A., ... & Jarrard, D. F. (2000). Methylation of the androgen receptor minimal promoter silences transcription in human prostate cancer. *Cancer research*, *60*(13), 3623-3630.

Kouzarides, T. (2007). Chromatin modifications and their function. *Cell*, *128*(4), 693-705.

Langmead, B., Trapnell, C., Pop, M., & Salzberg, S. L. (2009). Ultrafast and memory-efficient alignment of short DNA sequences to the human genome. *Genome Biol*, *10*(3), R25.

Laufer, M., Denmeade, S. R., SINIBALDI, V. J., CARDUCCI, M. A., & EISENBERGER, M. A. (2000). Complete androgen blockade for prostate cancer: what went wrong?. *The Journal of urology*, *164*(1), 3-9.

Lee, O. H., Kim, H., He, Q., Baek, H. J., Yang, D., Chen, L. Y., ... & Songyang, Z. (2011). Genome-wide YFP fluorescence complementation screen identifies new regulators for telomere signaling in human cells. *Molecular & Cellular Proteomics*, *10*(2), M110-001628.

Leiblich, A., Cross, S. S., Catto, J. W., Pesce, G., Hamdy, F. C., & Rehman, I. (2007). Human prostate cancer cells express neuroendocrine cell markers PGP 9.5 and chromogranin A. *The Prostate*, *67*(16), 1761-1769.

Leroy, E., Boyer, R., Auburger, G., Leube, B., Ulm, G., Mezey, E., ... & Polymeropoulos, M. H. (1998). The ubiquitin pathway in Parkinson's disease. *Nature*, *395*(6701), 451-452.

Li, L., Tao, Q., Jin, H., van Hasselt, A., Poon, F. F., Wang, X., ... & Cao, Y. (2010). The tumor suppressor UCHL1 forms a complex with p53/MDM2/ARF to promote p53 signaling and is frequently silenced in nasopharyngeal carcinoma. *Clinical Cancer Research*, *16*(11), 2949-2958.

Lin, K. W., & Yan, J. (2008). Endings in the middle: current knowledge of interstitial telomeric sequences. *Mutation Research/Reviews in Mutation Research*, *658*(1), 95-110.

Liu, D., O'Connor, M. S., Qin, J., & Songyang, Z. (2004). Telosome, a mammalian telomere-associated complex formed by multiple telomeric proteins. *Journal of Biological Chemistry*, *279*(49), 51338-51342.

Liu, L., Li, Y., Li, S., Hu, N., He, Y., Pong, R., ... & Law, M. (2012). Comparison of next-generation sequencing systems. *BioMed Research International*, *2012*.

Liu, Y., Fallon, L., Lashuel, H. A., Liu, Z., & Lansbury Jr, P. T. (2002). The UCH-L1 gene encodes two opposing enzymatic activities that affect α-synuclein degradation and Parkinson's disease susceptibility. *Cell*, *111*(2), 209-218.

Ma, Y., Zhao, M., Zhong, J., Shi, L., Luo, Q., Liu, J., ... & Huang, C. (2010). Proteomic profiling of proteins associated with lymph node metastasis in colorectal cancer. *Journal of cellular biochemistry*, *110*(6), 1512-1519.

Machida, Y. J., Machida, Y., Vashisht, A. A., Wohlschlegel, J. A., & Dutta, A. (2009). The deubiquitinating enzyme BAP1 regulates cell growth via interaction with HCF-1. *Journal of Biological Chemistry*, *284*(49), 34179-34188.

Mallery, D. L., Vandenberg, C. J., & Hiom, K. (2002). Activation of the E3 ligase function of the BRCA1/BARD1 complex by polyubiquitin chains. *The EMBO journal*, *21*(24), 6755-6762.

Mardis, E. R. (2008a). The impact of next-generation sequencing technology on genetics. *Trends in genetics*, *24*(3), 133-141.

Mardis, E. R. (2008b). Next-generation DNA sequencing methods. *Annu. Rev. Genomics Hum. Genet.*, *9*, 387-402.

Mardis, E. R. (2013). Next-generation sequencing platforms. *Annual review of analytical chemistry*, *6*, 287-303.

Martínez, P., & Blasco, M. A. (2010). Role of shelterin in cancer and aging. *Aging cell*, *9*(5), 653-666.

Mastoraki, A., Ioannidis, E., Apostolaki, A., Patsouris, E., & Aroni, K. (2009). PGP 9.5 and cyclin D1 coexpression in cutaneous squamous cell carcinomas. *International journal of surgical pathology*, *17*(6), 413-420.

Misaghi, S., Ottosen, S., Izrael-Tomasevic, A., Arnott, D., Lamkanfi, M., Lee, J., ... & Wilson, A. C. (2009). Association of C-terminal ubiquitin hydrolase BRCA1-associated protein 1 with cell cycle regulator host cell factor 1. *Molecular and cellular biology*, *29*(8), 2181-2192.

Mitchell, T. R., & Zhu, X. D. (2014). Methylated TRF2 associates with the nuclear matrix and serves as a potential biomarker for cellular senescence. *Aging (Albany NY)*, *6*(4), 248.

Mitsui, Y., Shiina, H., Hiraki, M., Arichi, N., Hiraoka, T., Sumura, M., ... & Igawa, M. (2012). Tumor Suppressor Function of PGP9. 5 Is Associated with Epigenetic Regulation in Prostate Cancer—Novel Predictor of Biochemical Recurrence after Radical Surgery. *Cancer Epidemiology Biomarkers & Prevention*, *21*(3), 487-496.

Miyashita, T., & Reed, J. C. (1995). Tumor suppressor p53 is a direct transcriptional activator of the human bax gene. *Cell*, *80*(2), 293-299.

Miyoshi, Y., Nakayama, S., Torikoshi, Y., Tanaka, S., Ishihara, H., Taguchi, T., ... & Noguchi, S. (2006). High expression of ubiquitin carboxy-terminal hydrolase-L1 and-L3 mRNA predicts early recurrence in patients with invasive breast cancer. *Cancer science*, *97*(6), 523-529.

Nishikawa, H., Wu, W., Koike, A., Kojima, R., Gomi, H., Fukuda, M., & Ohta, T. (2009). BRCA1-associated protein 1 interferes with BRCA1/BARD1 RING heterodimer activity. *Cancer research*, *69*(1), 111-119.

Osaka, H., Wang, Y. L., Takada, K., Takizawa, S., Setsuie, R., Li, H., ... & Wada, K. (2003). Ubiquitin carboxy-terminal hydrolase L1 binds to and stabilizes monoubiquitin in neuron. *Human Molecular Genetics*, *12*(16), 1945-1958.

Polascik, T. J., Oesterling, J. E., & Partin, A. W. (1999). Prostate specific antigen: a decade of discovery-what we have learned and where we are going. *The Journal of urology*, *162*(2), 293-306.

Pucci, B., Kasten, M., & Giordano, A. (2000). Cell cycle and apoptosis. *Neoplasia (New York, NY)*, *2*(4), 291.

Robinson, J. T., Thorvaldsdóttir, H., Winckler, W., Guttman, M., Lander, E. S., Getz, G., & Mesirov, J. P. (2011). Integrative genomics viewer. *Nature biotechnology*, *29*(1), 24-26.

Samuel, S. K., Spencer, V. A., Bajno, L., Sun, J. M., Holth, L. T., Oesterreich, S., & Davie, J. R. (1998). In situ cross-linking by cisplatin of nuclear matrix-bound transcription factors to nuclear DNA of human breast cancer cells. *Cancer research*, *58*(14), 3004-3008.

Scheuermann, J. C., de Ayala Alonso, A. G., Oktaba, K., Ly-Hartig, N., McGinty, R. K., Fraterman, S., ... & Müller, J. (2010). Histone H2A deubiquitinase activity of the Polycomb repressive complex PR-DUB. *Nature*, *465*(7295), 243-247.

Schnell, J. D., & Hicke, L. (2003). Non-traditional functions of ubiquitin and ubiquitin-binding proteins. *Journal of Biological Chemistry*, *278*(38), 35857-35860.

Seruga, B., Ocana, A., & Tannock, I. F. (2011). Drug resistance in metastatic castration-resistant prostate cancer. *Nature reviews Clinical oncology*, *8*(1), 12-23.

Setsuie, R., Sakurai, M., Sakaguchi, Y., & Wada, K. (2009). Ubiquitin dimers control the hydrolase activity of UCH-L3. *Neurochemistry international*, *54*(5), 314-321.

Sfeir, A. (2012). Telomeres at a glance. *Journal of cell science*, *125*(18), 4173-4178.

Shaw, G., Morse, S., Ararat, M., & Graham, F. L. (2002). Preferential transformation of human neuronal cells by human adenoviruses and the origin of HEK 293 cells. *The FASEB Journal*, *16*(8), 869-871.

Shiio, Y., & Eisenman, R. N. (2003). Histone sumoylation is associated with transcriptional repression. *Proceedings of the National Academy of Sciences*, *100*(23), 13225-13230.

Shin, H., Liu, T., Manrai, A. K., & Liu, X. S. (2009). CEAS: cis-regulatory element annotation system. *Bioinformatics*, *25*(19), 2605-2606.

Siedlecki, P., & Zielenkiewicz, P. (2006). Mammalian DNA methyltransferases. *ACTA BIOCHIMICA POLONICA-ENGLISH EDITION-*, *53*(2), 245.

Simonet, T., Zaragosi, L. E., Philippe, C., Lebrigand, K., Schouteden, C., Augereau, A., ... & Gilson, E. (2011). The human TTAGGG repeat factors 1 and 2 bind to a subset of interstitial telomeric sequences and satellite repeats. *Cell research*, *21*(7), 1028-1038.

Stone, K. R., Mickey, D. D., Wunderli, H., Mickey, G. H., & Paulson, D. F. (1978). Isolation of a human prostate carcinoma cell line (DU 145). *International journal of cancer*, *21*(3), 274-281.

Tezel, E., Hibi, K., Nagasaka, T., & Nakao, A. (2000). PGP9. 5 as a prognostic factor in pancreatic cancer. *Clinical Cancer Research*, *6*(12), 4764-4767.

Thalmann, G. N., Anezinis, P. E., Chang, S. M., Zhau, H. E., Kim, E. E., Hopwood, V. L., ... & Chung, L. W. (1994). Androgen-independent cancer progression and bone metastasis in the LNCaP model of human prostate cancer. *Cancer research*, *54*(10), 2577-2581.

Tokumaru, Y., Yamashita, K., Kim, M. S., Park, H. L., Osada, M., Mori, M., & Sidransky, D. (2008). The role of PGP9. 5 as a tumor suppressor gene in human cancer. *International journal of cancer*, *123*(4), 753-759.

Tsai, H. C., & Baylin, S. B. (2011). Cancer epigenetics: linking basic biology to clinical medicine. *Cell research*, *21*(3), 502-517.

Tyagi, S., Chabes, A. L., Wysocka, J., & Herr, W. (2007). E2F activation of S phase promoters via association with HCF-1 and the MLL family of histone H3K4 methyltransferases. *Molecular cell*, *27*(1), 107-119.

Ummanni, R., Jost, E., Braig, M., Lohmann, F., Mundt, F., Barett, C., ... & Balabanov, S. (2011). Ubiquitin carboxyl-terminal hydrolase 1 (UCHL1) is a potential tumour suppressor in prostate cancer and is frequently silenced by promoter methylation. *Molecular cancer*, *10*(1), 129.

Van Steensel, B., & De Lange, T. (1997). Control of telomere length by the human telomeric protein TRF1. *Nature*, 385-740.

Virnau, P., Mirny, L. A., & Kardar, M. (2006). Intricate knots in proteins: Function and evolution. *PLoS computational biology*, *2*(9), e122.

Wada, H., Kito, K., Caskey, L. S., Yeh, E. T., & Kamitani, T. (1998). Cleavage of the C-terminus of NEDD8 by UCH-L3. *Biochemical and biophysical research communications*, *251*(3), 688-692.

Walton, T. J., Li, G., Seth, R., McArdle, S. E., Bishop, M. C., & Rees, R. C. (2008). DNA demethylation and histone deacetylation inhibition co-operate to re-express estrogen receptor beta and induce apoptosis in prostate cancer cell-lines. *The Prostate*, *68*(2), 210-222.

Wang, X. W., Vermeulen, W., Coursen, J. D., Gibson, M., Lupold, S. E., Forrester, K., ... & Harris, C. C. (1996). The XPB and XPD DNA helicases are components of the p53-mediated apoptosis pathway. *Genes & development*, *10*(10), 1219-1232.

Wang, X., He, S., Sun, J. M., Delcuve, G. P., & Davie, J. R. (2010). Selective association of peroxiredoxin 1 with genomic DNA and COX-2 upstream promoter elements in estrogen receptor negative breast cancer cells. *Molecular biology of the cell*, *21*(17), 2987-2995.

Wilkinson, K. D. (2000, June). Ubiquitination and deubiquitination: targeting of proteins for degradation by the proteasome. In *Seminars in cell & developmental biology* (Vol. 11, No. 3, pp. 141-148). Academic Press.

Wilkinson, K. D., Lee, K. M., Deshpande, S. E. E. M. A., Duerksen-Hughes, P., Boss, J. M., & Pohl, J. (1989). The neuron-specific protein PGP 9.5 is a ubiquitin carboxyl-terminal hydrolase. *Science*, *246*(4930), 670-673.

Xin, H., Liu, D., & Songyang, Z. (2008). The telosome/shelterin complex and its functions. *Genome Biol*, *9*(9), 232.

Yang, D., Xiong, Y., Kim, H., He, Q., Li, Y., Chen, R., & Songyang, Z. (2011). Human telomeric proteins occupy selective interstitial sites. *Cell research*, *21*(7), 1013-1027.

Yao, T., Song, L., Jin, J., Cai, Y., Takahashi, H., Swanson, S. K., ... & Conaway, J. W. (2008). Distinct modes of regulation of the Uch37 deubiquitinating enzyme in the proteasome and in the Ino80 chromatin-remodeling complex. *Molecular cell*, *31*(6), 909-917.

Yao, T., Song, L., Xu, W., DeMartino, G. N., Florens, L., Swanson, S. K., ... & Cohen, R. E. (2006). Proteasome recruitment and activation of the Uch37 deubiquitinating enzyme by Adrm1. *Nature cell biology*, *8*(9), 994-1002.

Yu, J., Tao, Q., Cheung, K. F., Jin, H., Poon, F. F., Wang, X., ... & Sung, J. J. (2008). Epigenetic identification of ubiquitin carboxyl-terminal hydrolase L1 as a functional tumor suppressor and biomarker for hepatocellular carcinoma and other digestive tumors. *Hepatology*, *48*(2), 508-518.

Zetterberg, M., Sjolander, A., von Otter, M., Palmér, M. S., Landgren, S., Minthon, L., ... & Palmér, M. S. (2010). Ubiquitin carboxy-terminal hydrolase L1 (UCHL1) S18Y polymorphism in Alzheimer's disease. *Molecular neurodegeneration*, *5*(1), 11.

Zhang, Y., Liu, T., Meyer, C. A., Eeckhoute, J., Johnson, D. S., Bernstein, B. E., ... & Liu, X. S. (2008). Model-based analysis of ChIP-Seq (MACS). *Genome Biol*, *9*(9), R137.